

830 **Supplementary Material**

831 **Contents**

- 832 1. Reconstruction gallery: Supplementary figures S1-S11
- 833 2. Supplementary qualitative automated reconstruction studies: Supp. figures S12-S15
- 834 3. Supplementary quantification of automated reconstruction: Supp. figures S16-S18
- 835 4. Supplementary cell type classification studies: Supp. figures S19-S21
- 836 5. Supplementary statistics of automated reconstruction accuracy: Supp. tables S1-S2
- 837 6. Supplementary statistics for the sparse gene selection study: Supp. tables S3-S4
- 838 7. Selected gene sets for different cell types/subclasses and anatomical features: Supp.
839 table S5

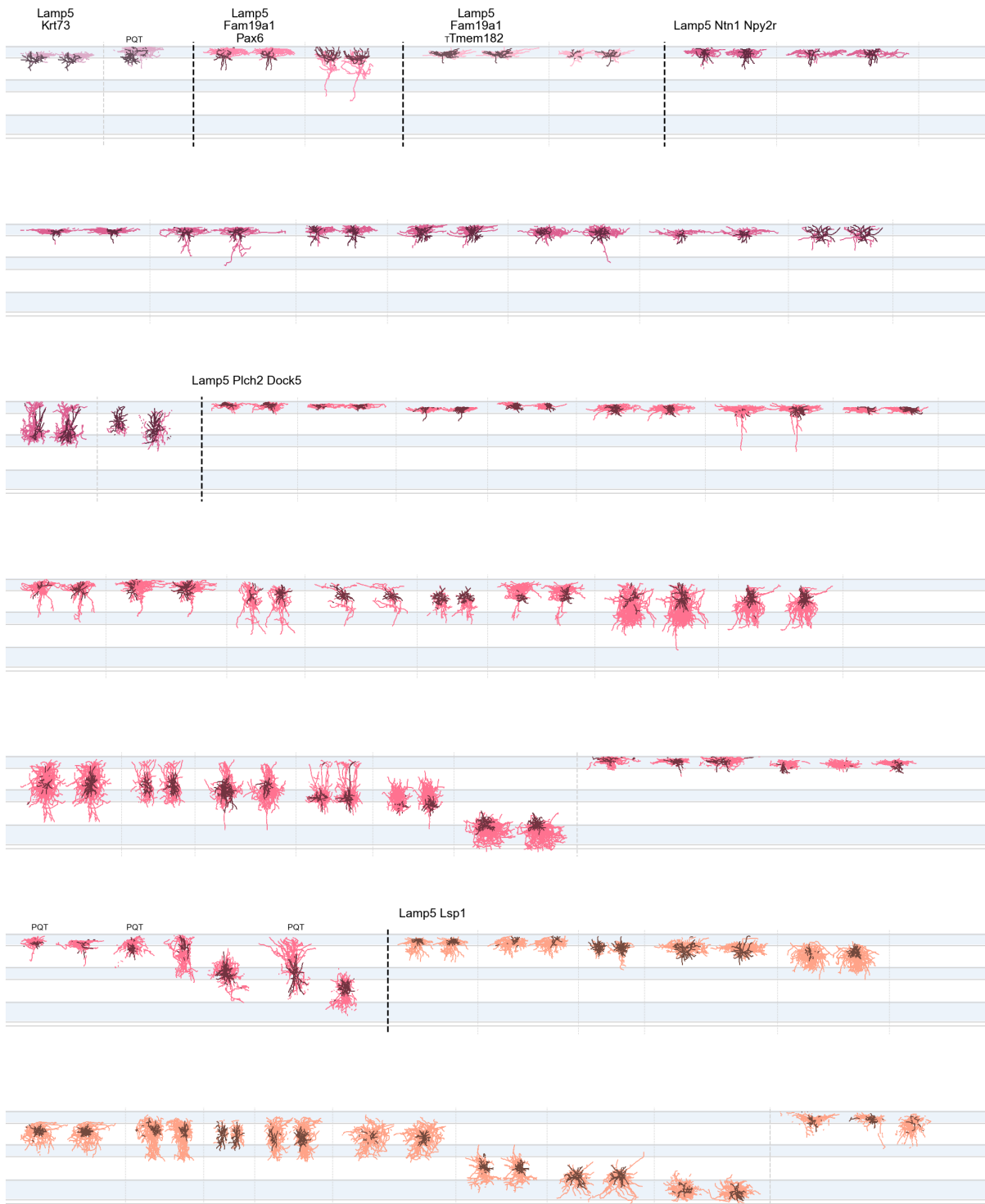


Figure S1: Morphological reconstructions of inhibitory neurons ordered by t-type – 1 of 11. $n=543$ neurons have both automated and manual reconstructions, $n=270$ - only automated ones. For each t-type, cells with both automated and manual reconstructions are shown first, separated by faint dashed lines, followed by cells that are reconstructed only automatically. Dendrites and axon are in darker and lighter colors, respectively. Best viewed digitally. PQT: poor quality transcriptomic characterization – not used for t-type related analyses. T: cells used in segmentation model training.

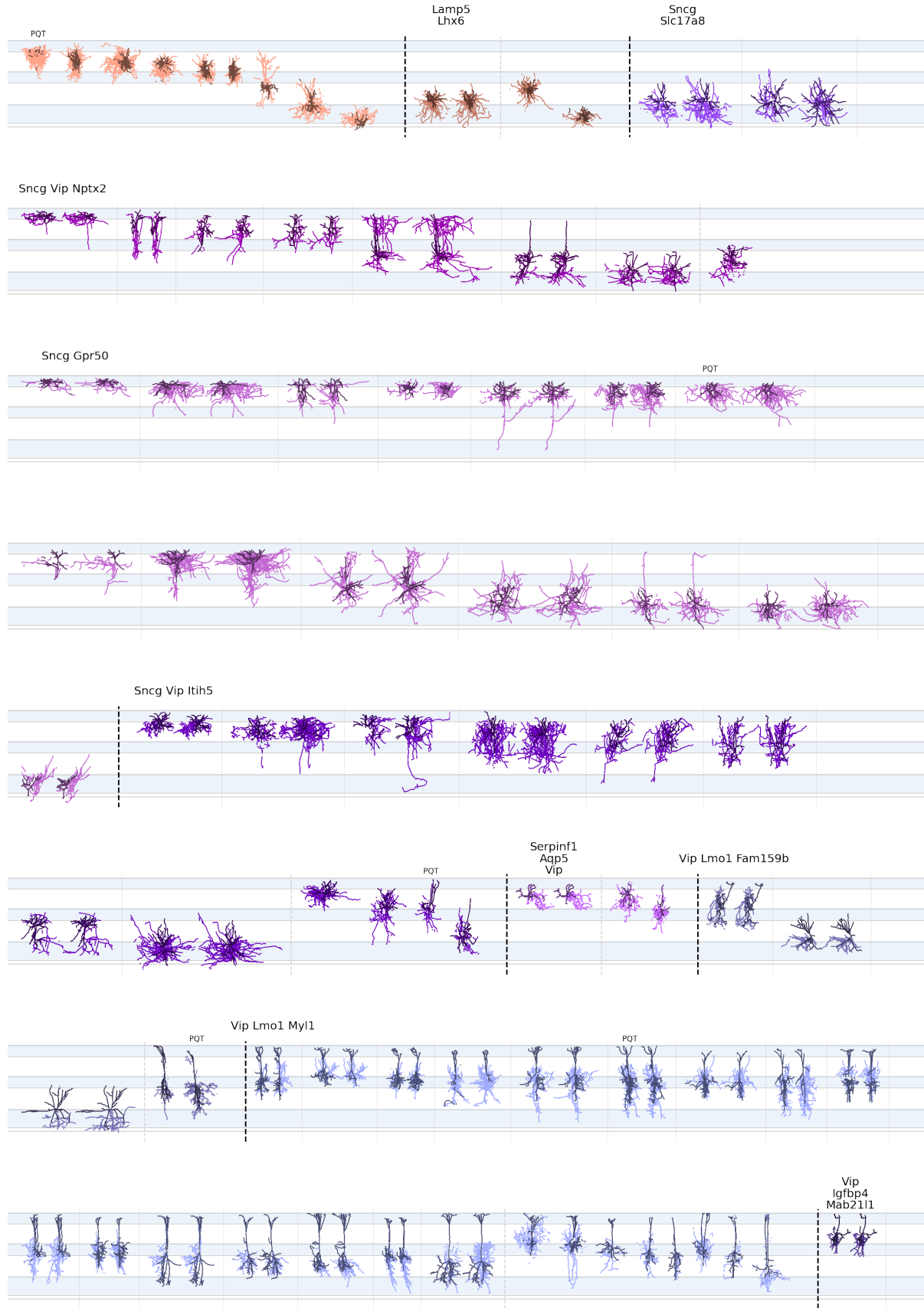


Figure S2: Morphological reconstructions of inhibitory neurons ordered by t-type – 2 of 11. Please refer to the caption of Figure S1.

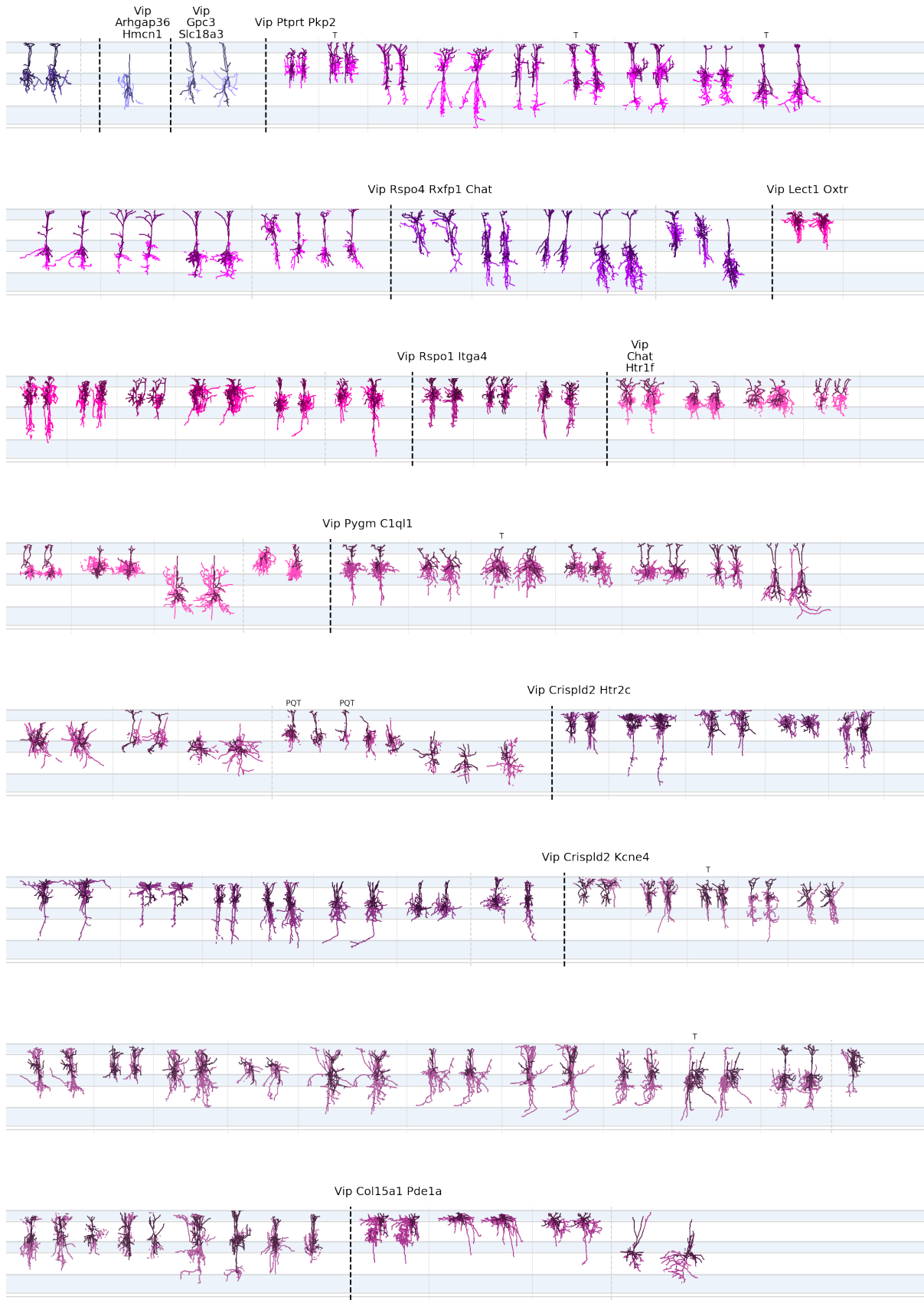
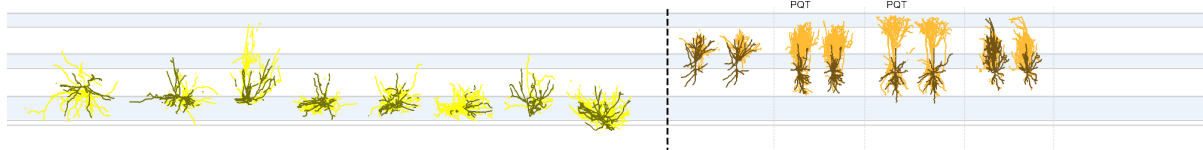


Figure S3: Morphological reconstructions of inhibitory neurons ordered by t-type – 3 of 11. Please refer to the caption of Figure S1.

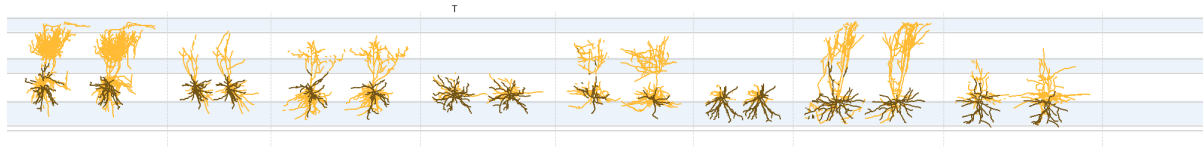
Sst Chodl



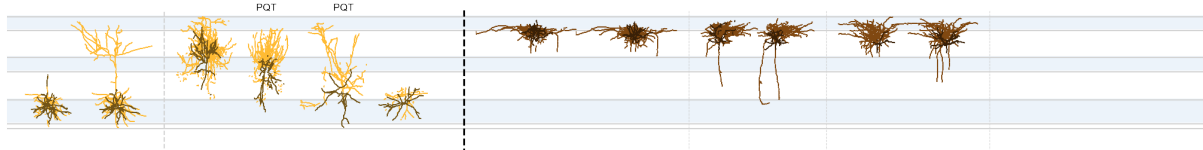
Sst Mme Fam114a1



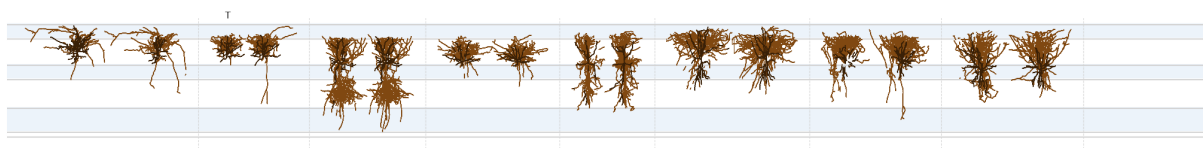
T



Sst Tac1 Htr1d



T



Sst Tac1 Tacr3



Figure S4: Morphological reconstructions of inhibitory neurons ordered by t-type – 4 of 11. Please refer to the caption of Figure S1.

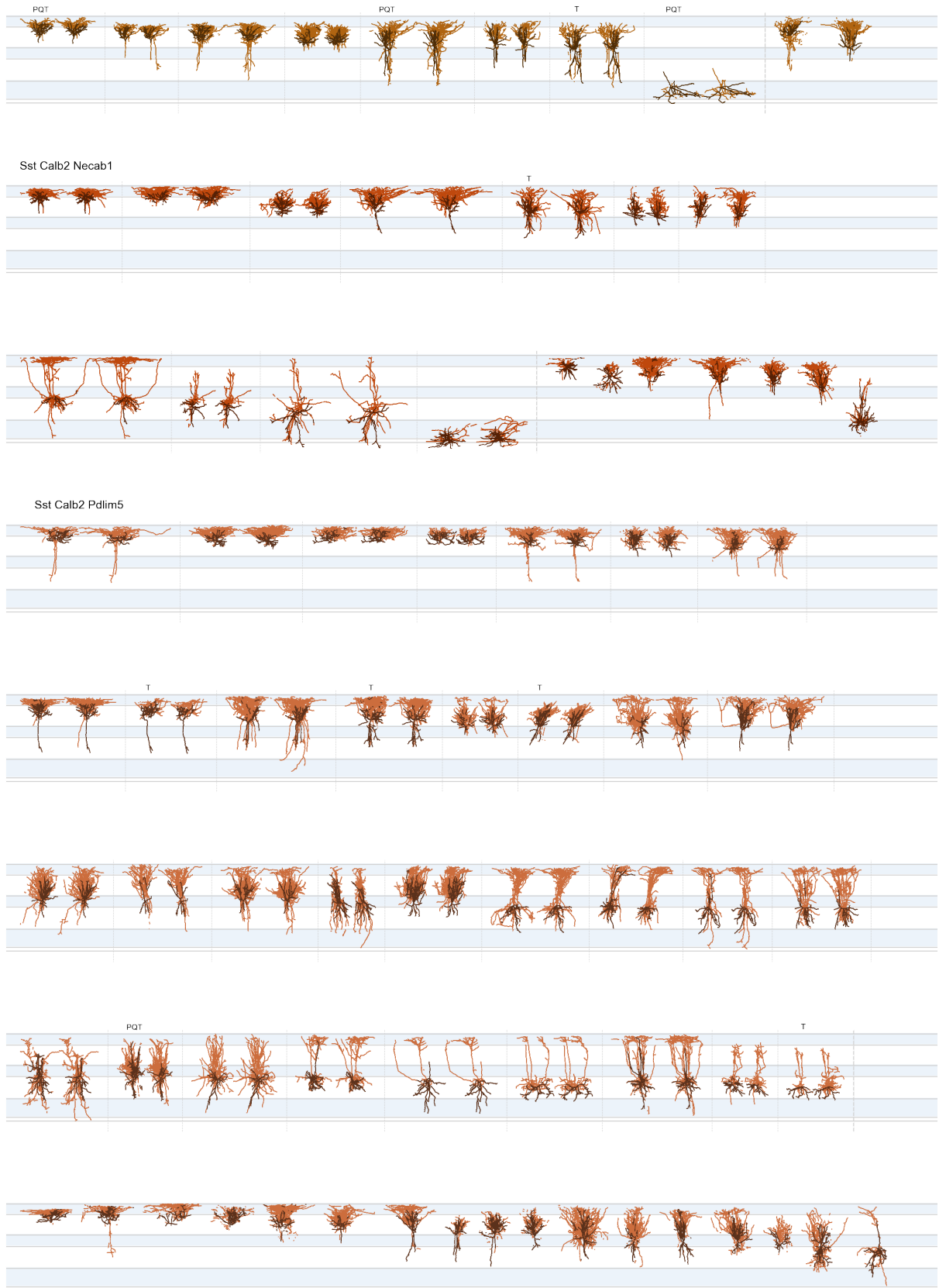


Figure S5: Morphological reconstructions of inhibitory neurons ordered by t-type – 5 of 11. Please refer to the caption of Figure S1.

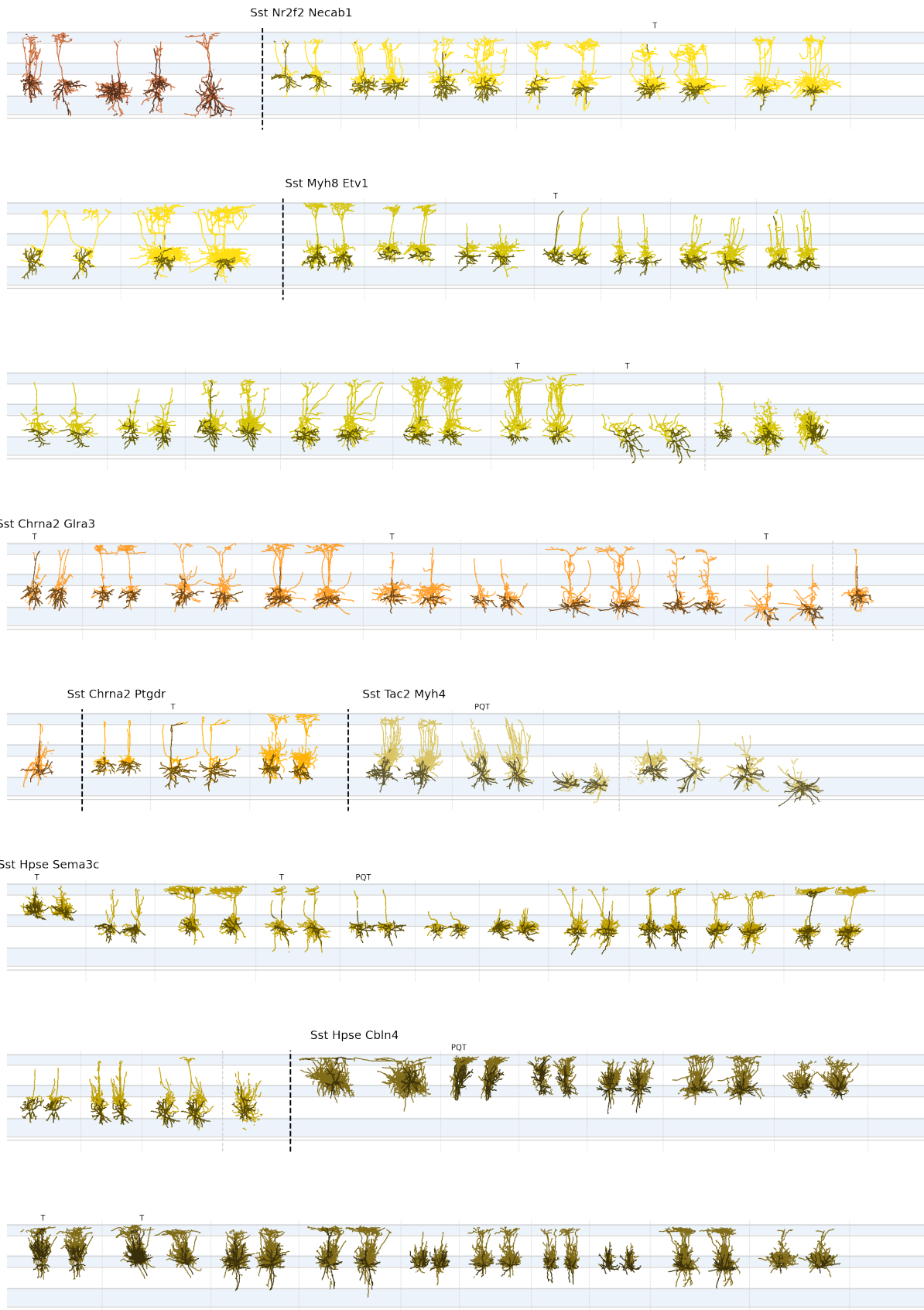


Figure S6: Morphological reconstructions of inhibitory neurons ordered by t-type – 6 of 11. Please refer to the caption of Figure S1.

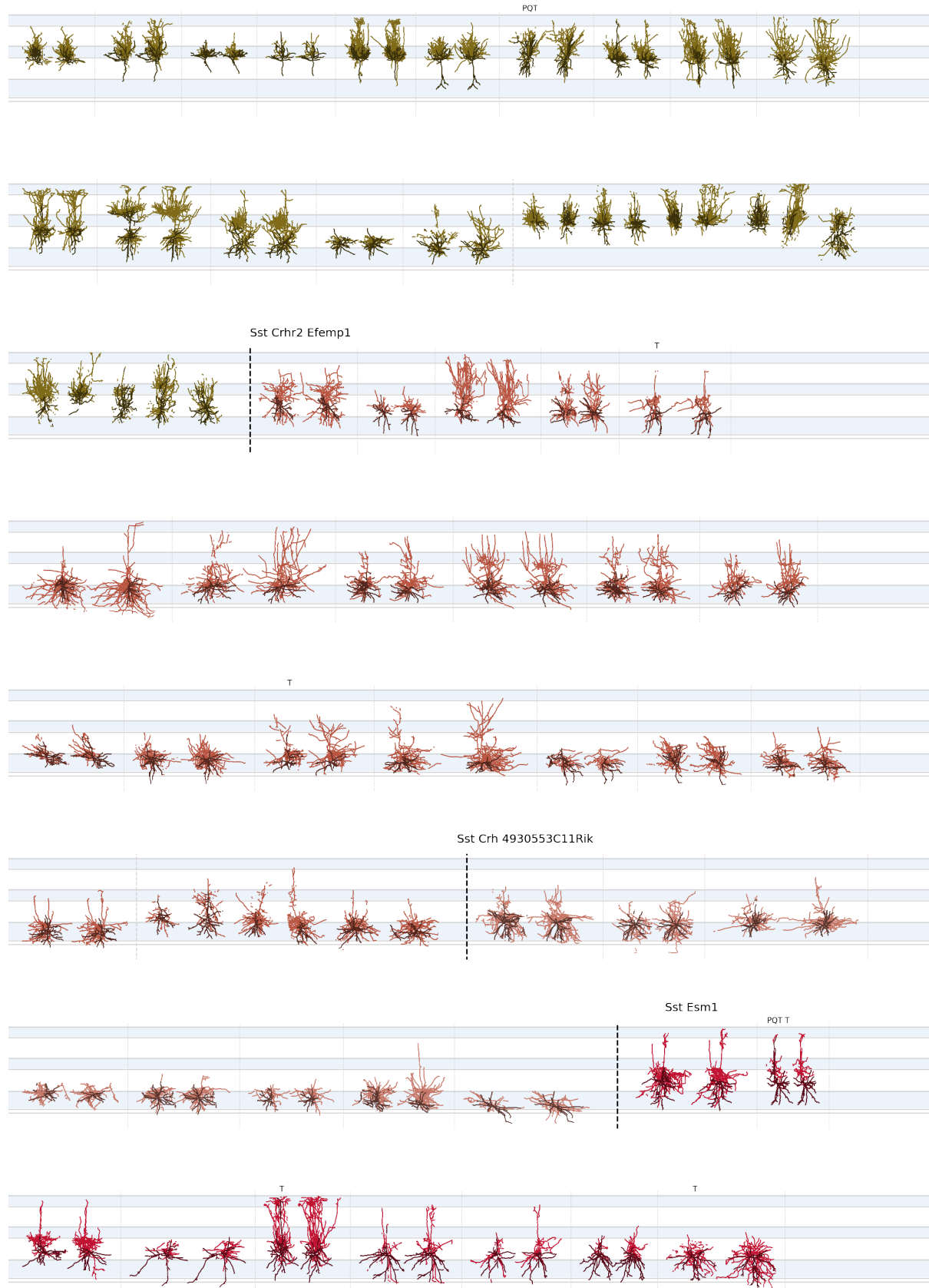


Figure S7: Morphological reconstructions of inhibitory neurons ordered by t-type – 7 of 11. Please refer to the caption of Figure S1.

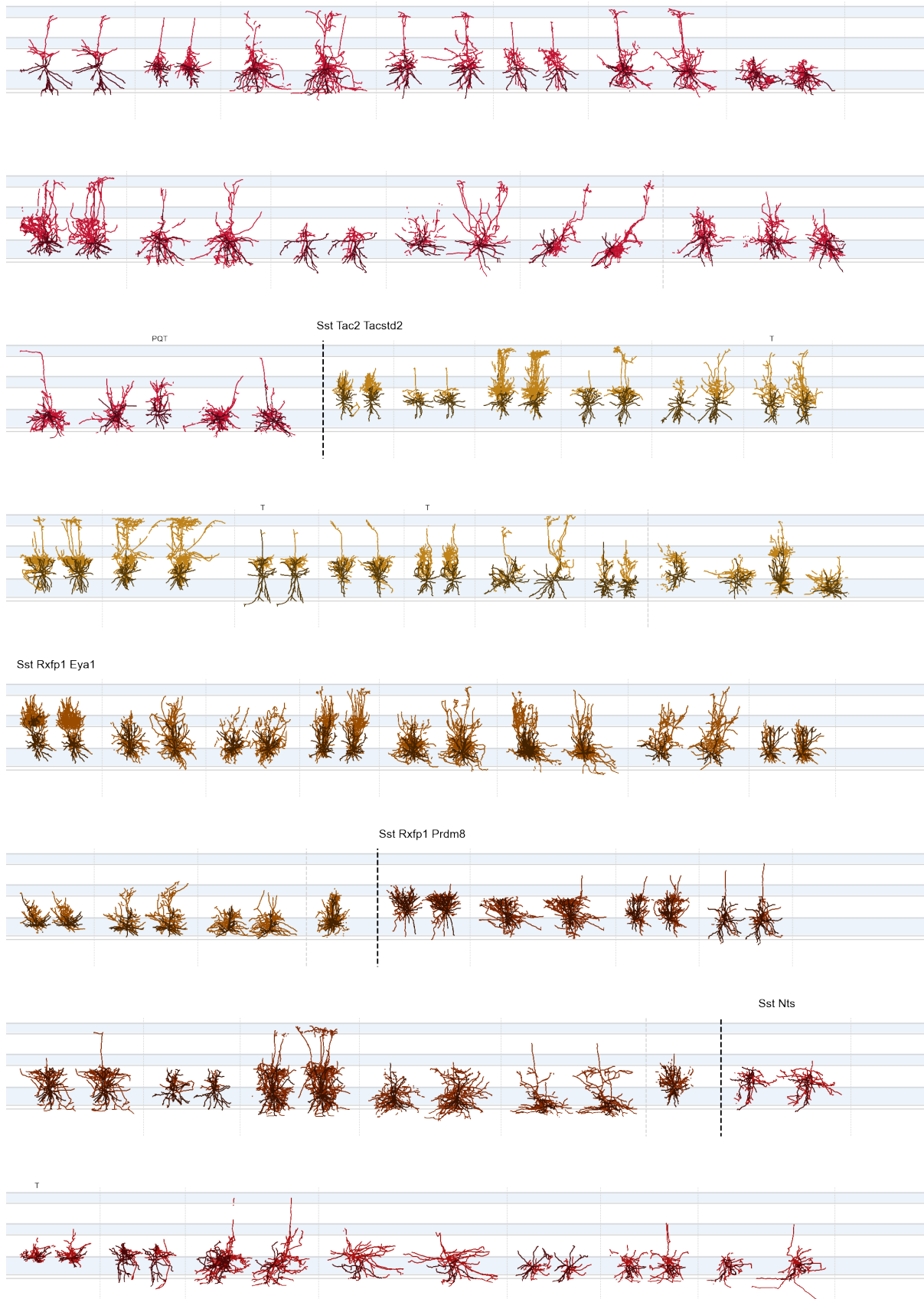


Figure S8: Morphological reconstructions of inhibitory neurons ordered by t-type – 8 of 11. Please refer to the caption of Figure S1.

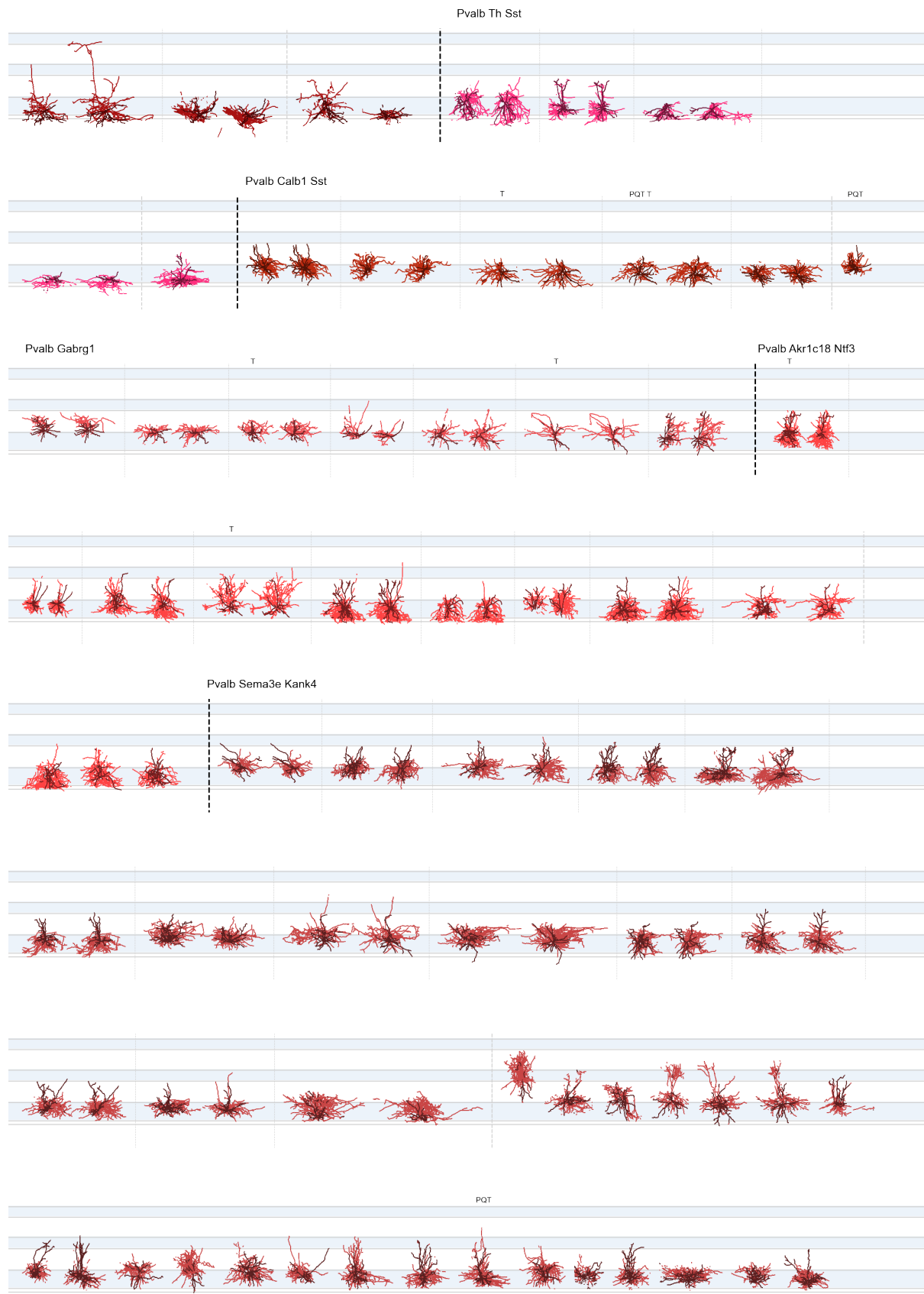


Figure S9: Morphological reconstructions of inhibitory neurons ordered by t-type – 9 of 11. Please refer to the caption of Figure S1.

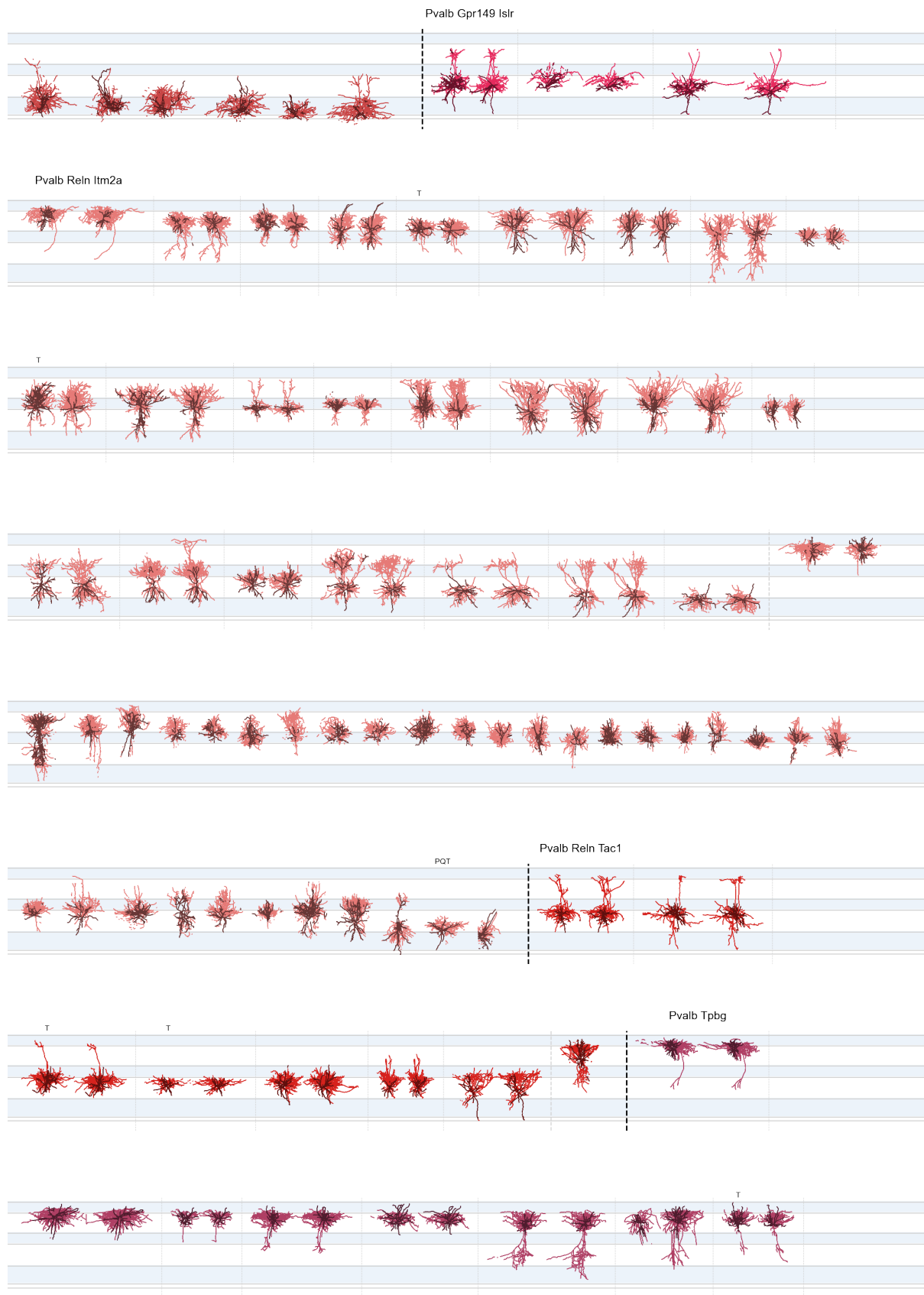


Figure S10: Morphological reconstructions of inhibitory neurons ordered by t-type – 10 of 11. Please refer to the caption of Figure S1.

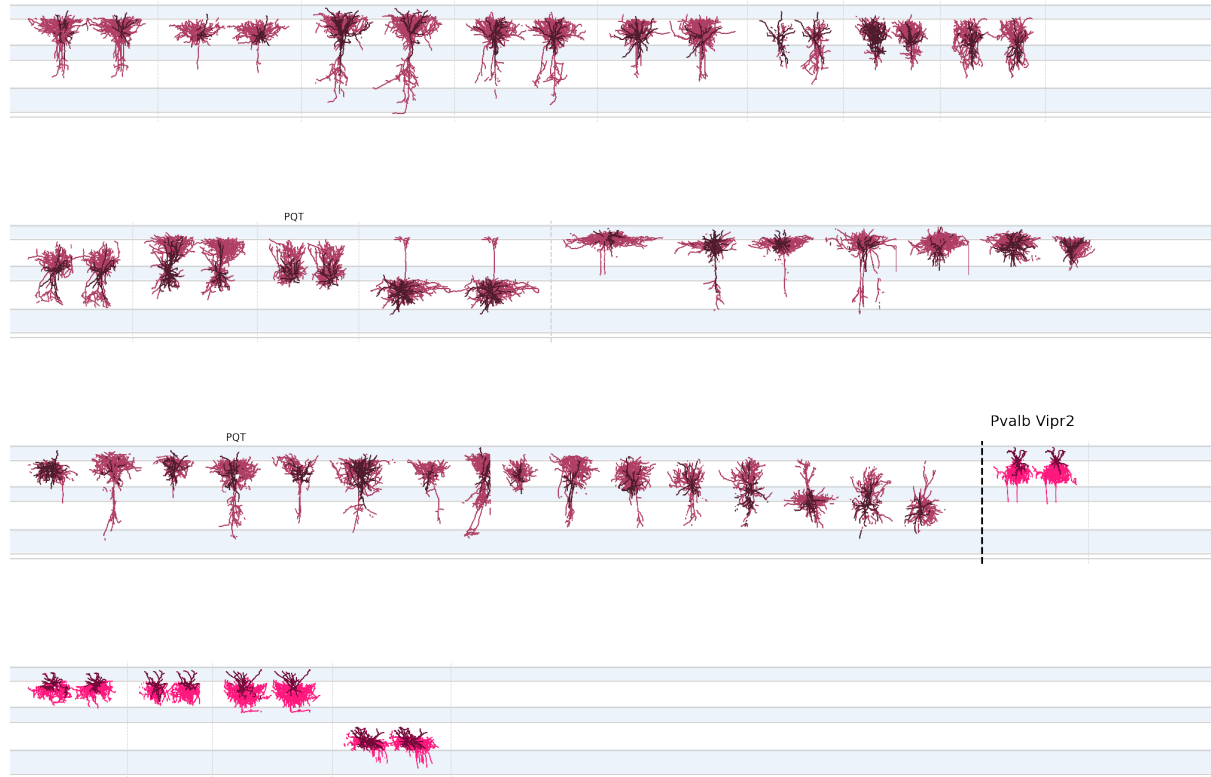


Figure S11: Morphological reconstructions of inhibitory neurons ordered by t-type – 11 of 11. Please refer to the caption of Figure S1.

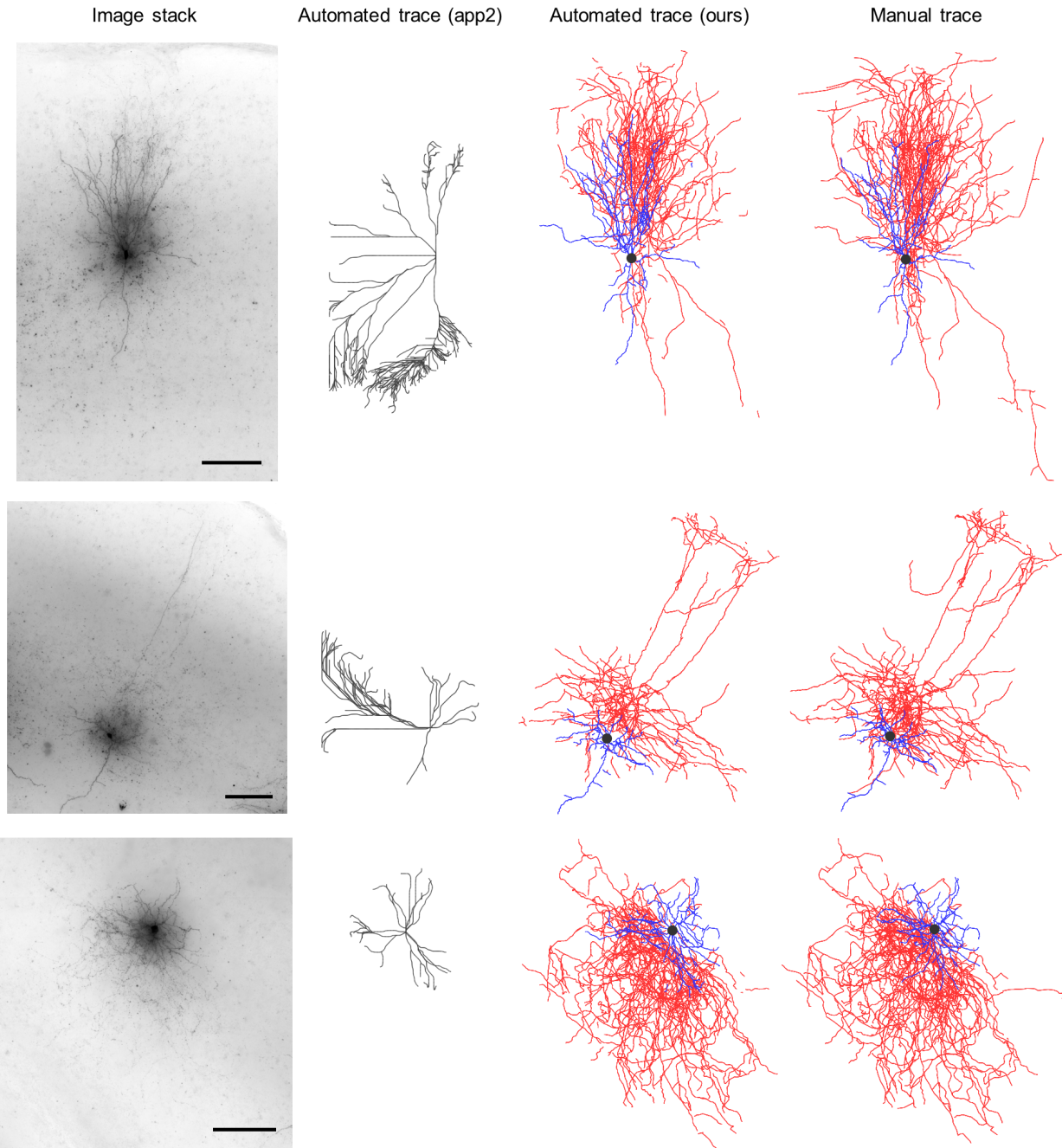


Figure S12: A qualitative comparative study of automated reconstruction accuracy based on three example test inhibitory neurons. Minimum intensity projection of image stacks (left column), automated reconstructions using the app2 algorithm^{[30][31]} (second column), automated reconstructions using the proposed method (third column), manual reconstructions (right column). We tried multiple parameter values to optimize app2's performance. For manual and our automated reconstructions: dendrites (blue), axons (red), soma (black). For automated reconstructions using app2: neurites (gray). Scale bar, 100 μm . Source data are provided as a Source Data file.

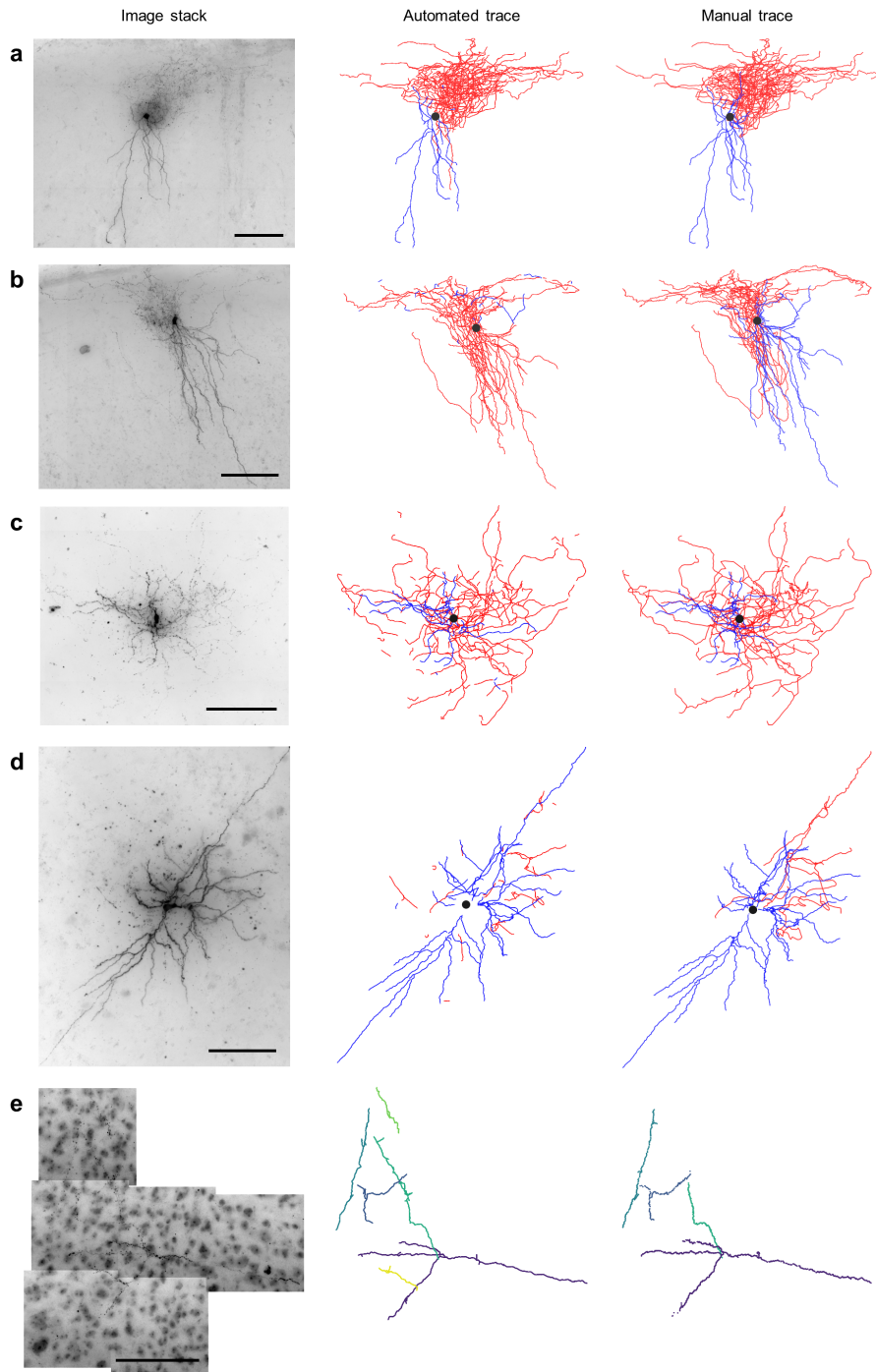


Figure S13: Morphological reconstructions of example neurons from other datasets, without tuning the segmentation model. Left column: minimum intensity projection of image stacks, middle column: automated reconstruction, right column: manual reconstruction. **a**, A human cortical inhibitory cell. **b**, Another human cortical inhibitory cell. All experimental steps prior to imaging were performed by a different laboratory and imaging was done at the Allen Institute^[32]). **c**, A macaque subcortical inhibitory cell. **d**, Mouse subcortical inhibitory cell. Dendrites (blue), axons (red), soma (black). **e**, Part of a cat cortical excitatory cell, a part of the DIADEM dataset,^[33] originally obtained by Ref.^[34] – different colors indicate different connected components. Scale bar, 100 μm . Source data are provided as a Source Data file.

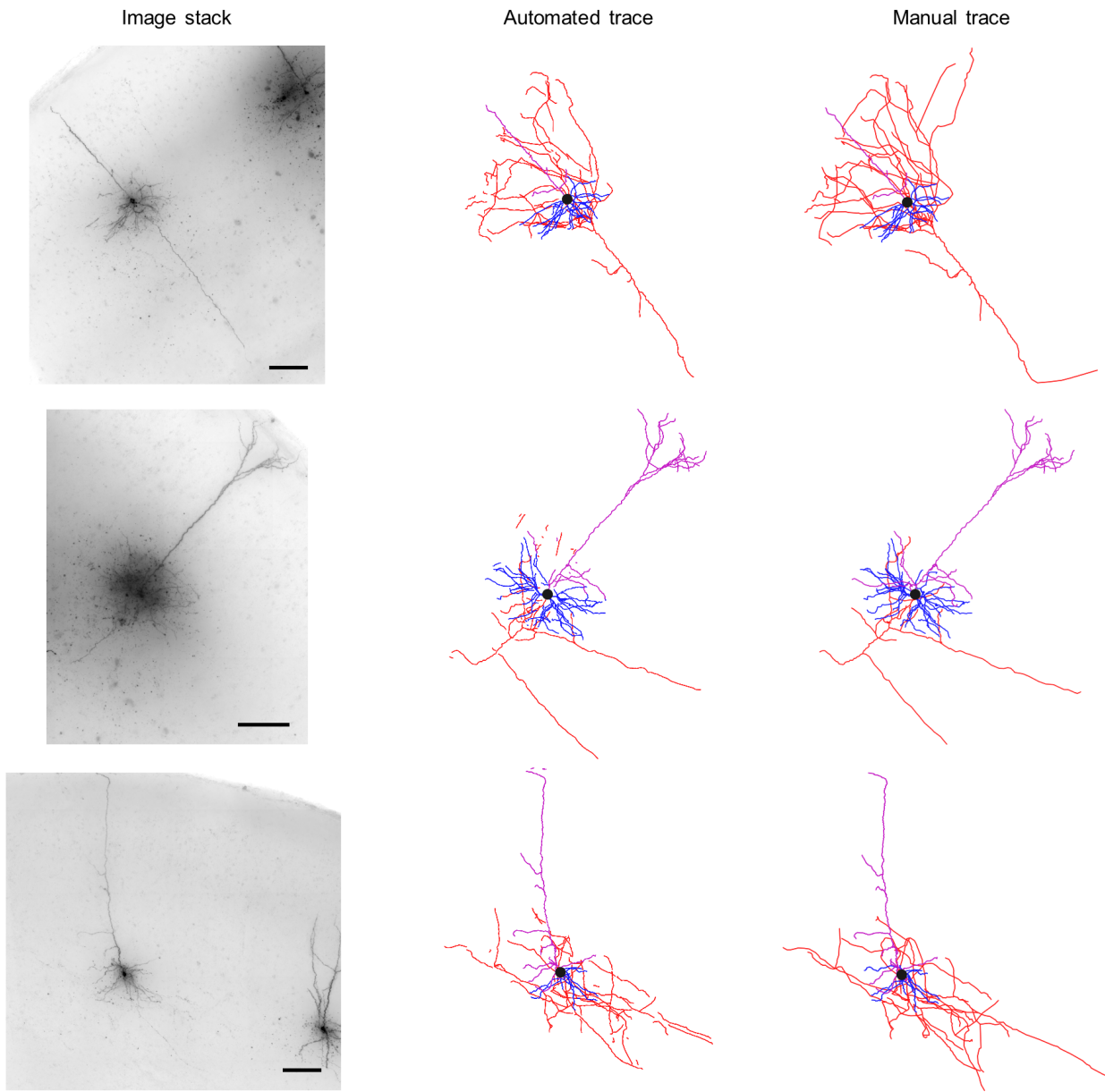


Figure S14: Morphological reconstructions of example excitatory neurons with traced axons. The method can trace and label the axon as well when it is captured in the slice. Minimum intensity projection of image stacks (left column), automated reconstructions (middle column), manual reconstructions (right column). Basal dendrites (blue), apical dendrites (magenta), axon (red), soma (black). Scale bar, 100 μm . Source data are provided as a Source Data file.

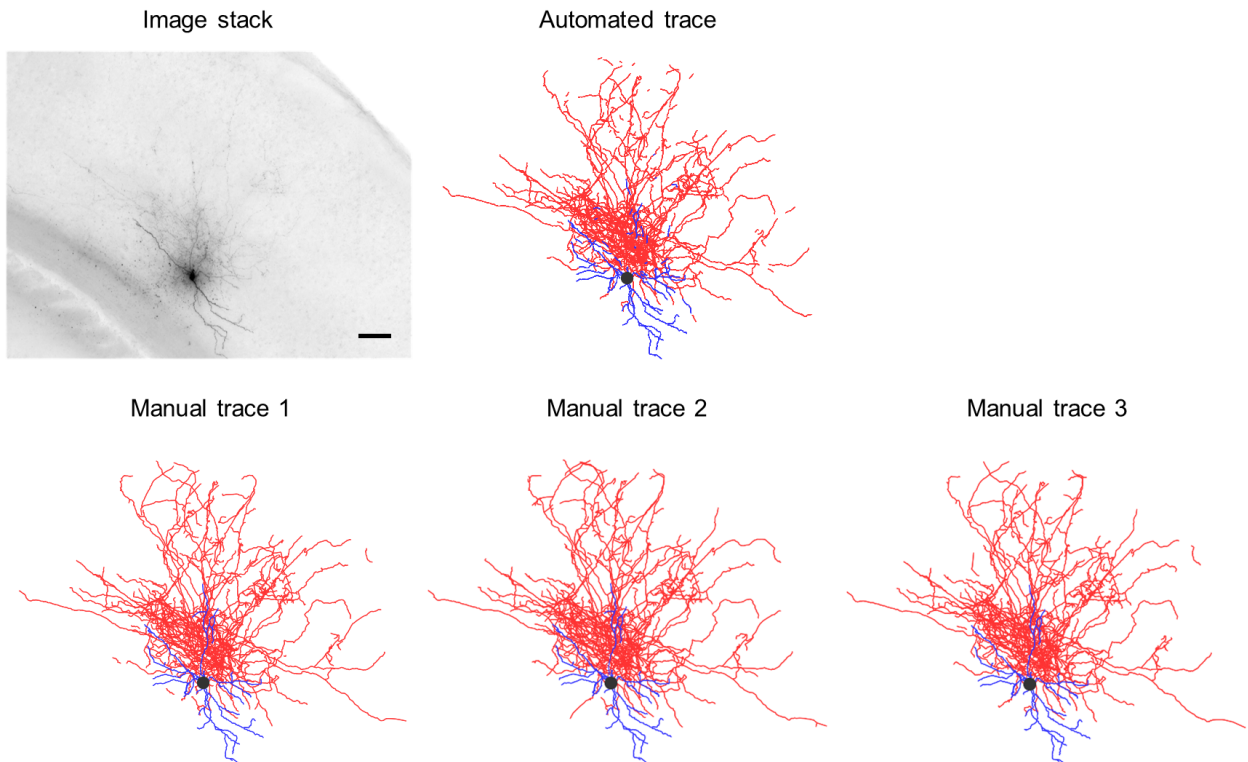


Figure S15: Comparison of automated vs. multiple manual reconstructions for one example test neuron. This neuron is not used for training. Multiple manual reconstructions are obtained to estimate cross-human agreement. Minimum intensity projection of the image stack (top left), automated reconstruction (top middle), manual reconstructions (bottom). Dendrites (blue), axons (red), soma (black). Scale bar, 100 μm . See Table S2 for quantification. Source data are provided as a Source Data file.

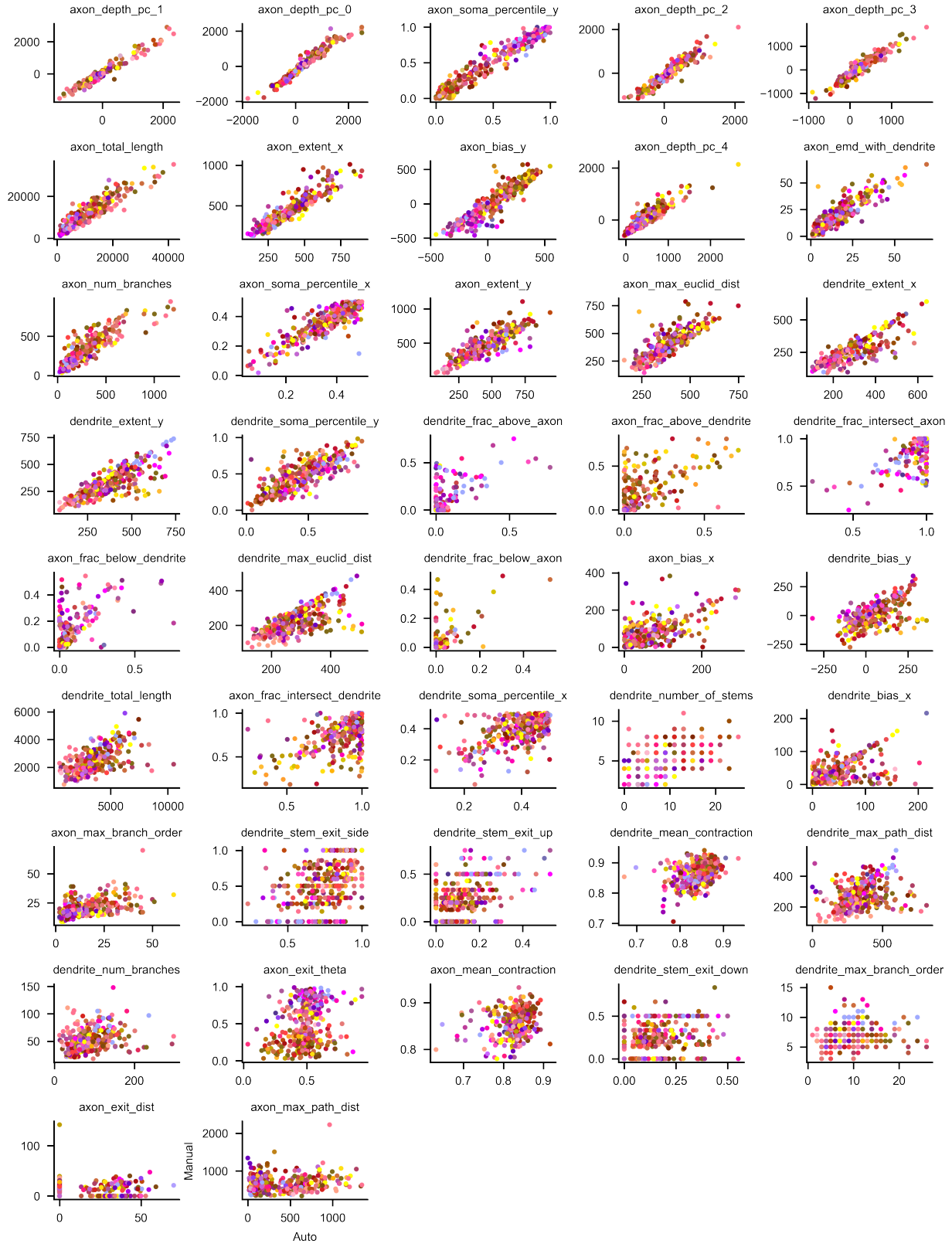


Figure S16: Comparison of automatically vs. manually generated morphometric features.
 Scatter plots ($n=340$ cells) for every feature are shown. For each feature, the y -axis denotes values based on manual traces and the x -axis denotes values based on automated traces. Each dot depicts an individual cell, and its color indicates the cell's t-type, consistent with the coloring scheme in Ref.^[5]
 Source data are provided as a Source Data file.

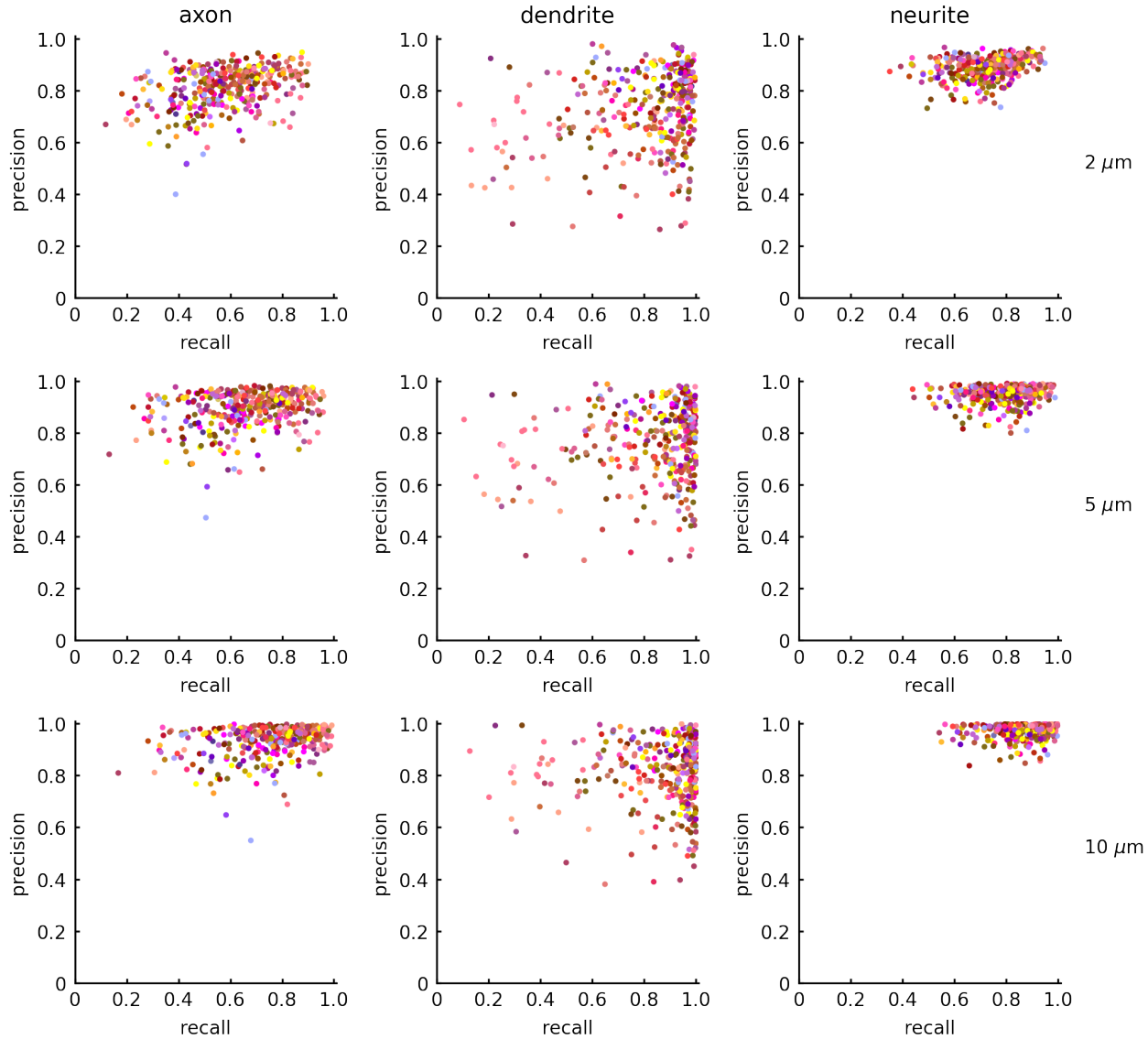


Figure S17: Neuron reconstruction accuracy. Scatter plots ($n=340$ cells) for precision vs. recall calculated by comparing automated and manual trace nodes within a given distance (2, 5, and 10 μm), as described in the main text, are shown for axonal, dendritic, and neurite (axonal or dendritic) nodes. Each dot depicts an individual cell, and its color indicates the cell's t-type, consistent with the coloring scheme in Ref.⁵ Source data are provided as a Source Data file.

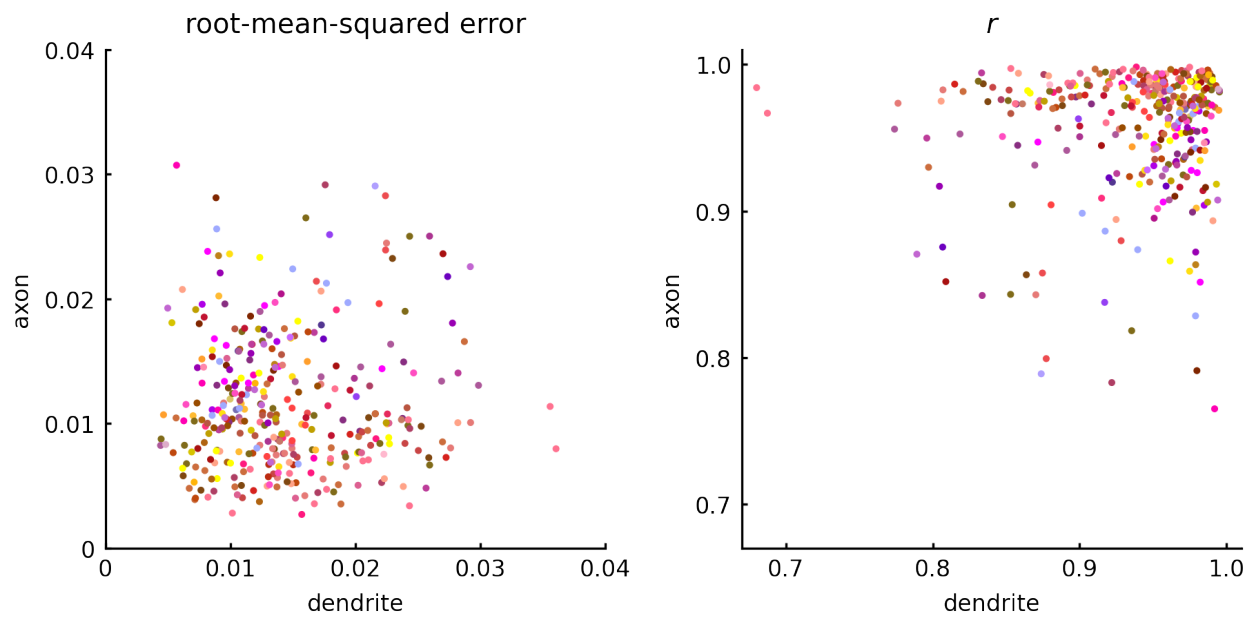


Figure S18: **Comparison of automatically vs. manually generated ADRs.** Scatter plots ($n=340$ cells) for the root-mean-squared error (left) and Pearson's correlation r values (right) for each cell's automatically reconstructed axonal vs. dendritic arbors, with respect to the corresponding manual traces, are shown. Each dot depicts an individual cell, and its color indicates the cell's t-type, consistent with the coloring scheme in Ref.⁵ Source data are provided as a Source Data file.

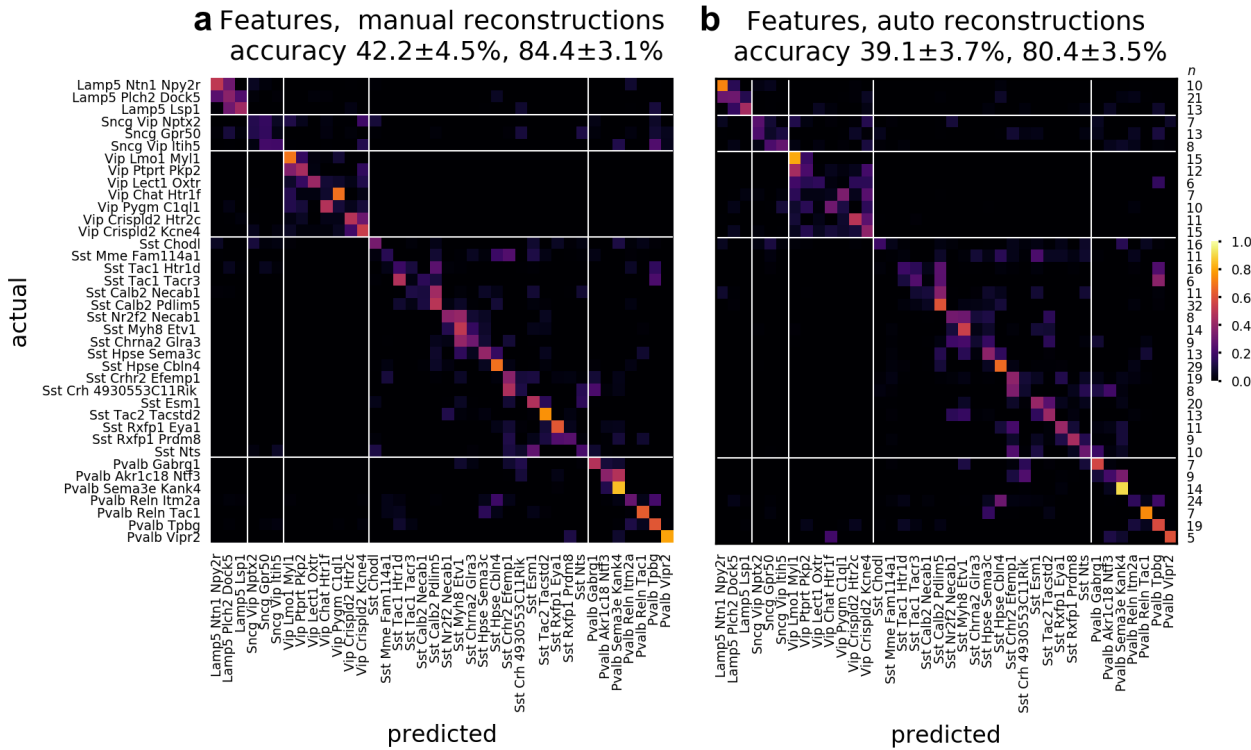


Figure S19: Comparison of cell type classification accuracy based on a set of classical morphometric features using manually vs. automatically reconstructed cells. Confusion matrix for the classification of 38 t-types based on features, using manually ($n=488$ cells) (a) and automatically ($n=488$ cells) (b) reconstructed cells. Accuracy values reported in the headers refer to mean \pm s.d. of the overall t-type and t-subclass classifiers, respectively, across cross-validation folds. Rightmost column lists the number of cells in each t-type (n). Source data are provided as a Source Data file.

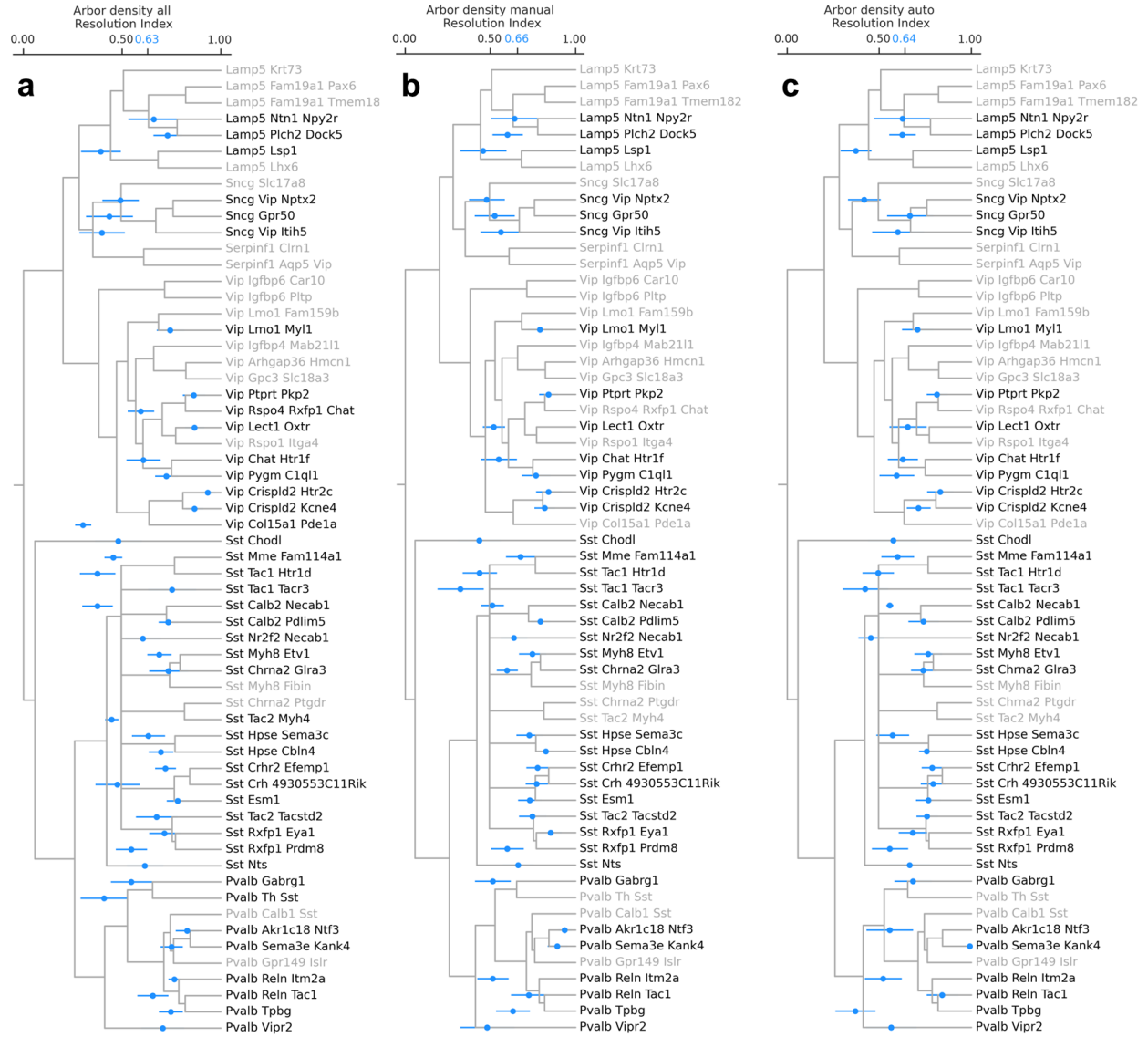


Figure S20: Arbor density-based cell type classification performance using resolution index.

The depth of the Tasic et al. GABAergic neuron hierarchical tree is normalized to the 0-1 range, and resolution index for each cell is defined as the value of the closest common ancestor of the true and predicted leaf node labels. Perfect classification corresponds to resolution index of 1. Error bars indicate resolution index (mean \pm SE over 10-fold stratified cross validation sets) for each cell type. The overall mean across cell types is indicated by blue on the *y*-axis. Cell types absent from the dataset are indicated by grayed out labels on the *x*-axis. Classification was performed with multi-layer perceptron classifiers using arbor density representation of all (a), manually (b) and automatically (c) reconstructed neurons as input. Resolution index values are not strictly comparable across panels because the numbers of cells and types are not identical. Left panel: $n=747$ cells, 42 types; middle and right panels: $n=488$ cells, 38 types. (See Figure 3.) Source data are provided as a Source Data file.

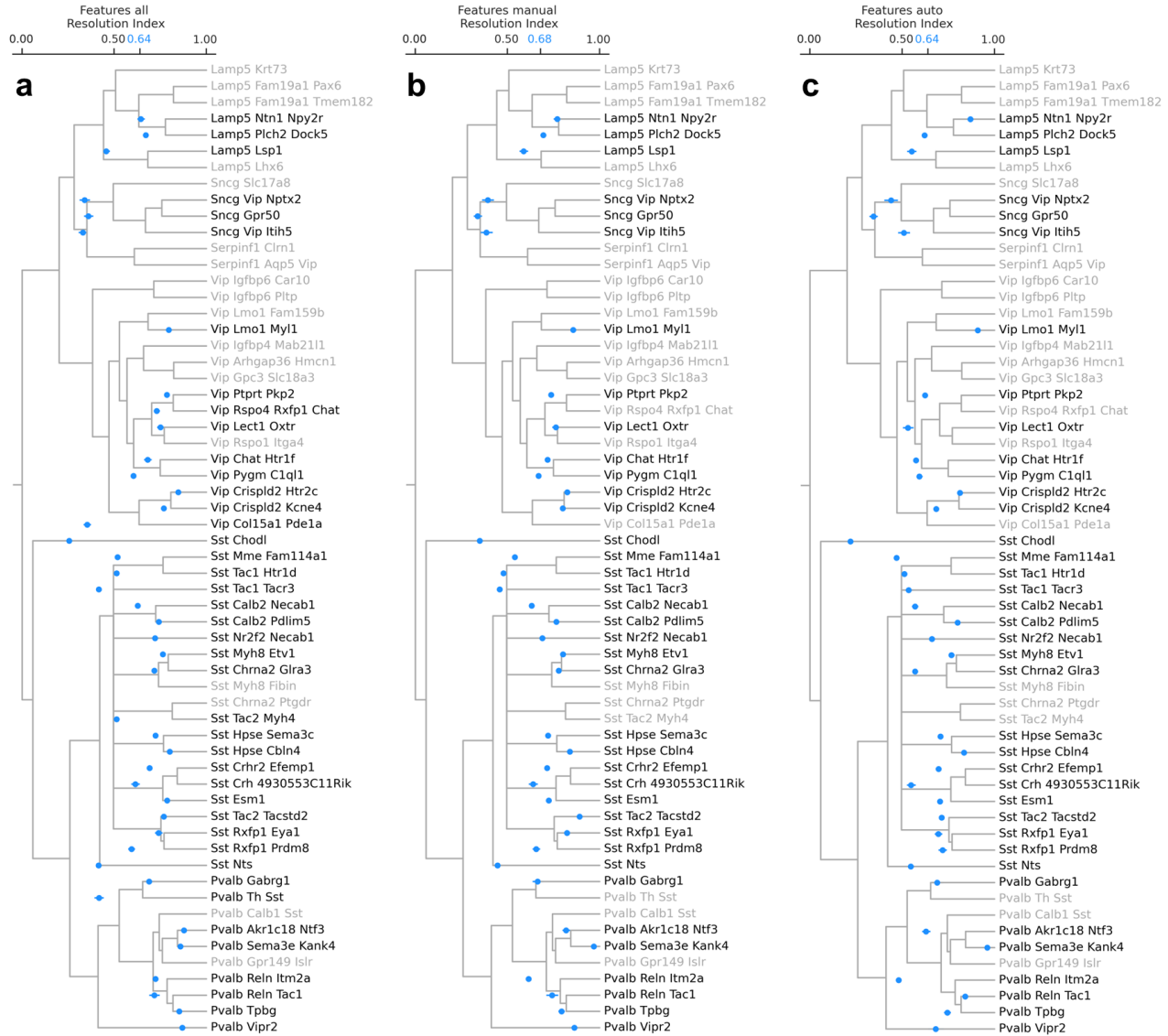


Figure S21: Feature-based cell type classification performance using resolution index. As before, error bars indicate resolution index (mean \pm SE over 5-fold stratified cross validation sets repeated 20 times) for each cell type. The overall mean across cell types is indicated by blue on the *y*-axis. Cell types absent from the dataset are indicated by grayed out labels on the *x*-axis. Classification was performed with random forest classifiers using morphometric features of all (**a**), manually (**b**) and automatically reconstructed cells (**c**) as input. Resolution index values are not strictly comparable across panels because the numbers of cells and types are not identical. Left panel: $n=747$ cells, 42 types; middle and right panels: $n=488$ cells, 38 types. (See Figure 3.) Source data are provided as a Source Data file.

| Precision | Axon | | Dendrite | | Neurite | |
|-------------------------|-----------------|-----------------|-----------------|-----------------|-----------------|-----------------|
| Distance, μm | raw | masked | raw | masked | raw | masked |
| 2 | 0.81 ± 0.08 | 0.83 ± 0.07 | 0.72 ± 0.15 | 0.73 ± 0.15 | 0.89 ± 0.04 | 0.91 ± 0.03 |
| 5 | 0.89 ± 0.07 | 0.91 ± 0.06 | 0.76 ± 0.14 | 0.77 ± 0.14 | 0.95 ± 0.03 | 0.97 ± 0.02 |
| 10 | 0.93 ± 0.06 | 0.96 ± 0.05 | 0.82 ± 0.12 | 0.82 ± 0.12 | 0.97 ± 0.03 | 0.99 ± 0.01 |

| Recall | Axon | | Dendrite | | Neurite | |
|-------------------------|-----------------|-----------------|-----------------|-----------------|-----------------|-----------------|
| Distance, μm | raw | masked | raw | masked | raw | masked |
| 2 | 0.58 ± 0.16 | 0.58 ± 0.16 | 0.81 ± 0.20 | 0.81 ± 0.20 | 0.73 ± 0.11 | 0.73 ± 0.11 |
| 5 | 0.66 ± 0.16 | 0.66 ± 0.16 | 0.83 ± 0.19 | 0.83 ± 0.19 | 0.80 ± 0.11 | 0.80 ± 0.11 |
| 10 | 0.75 ± 0.16 | 0.75 ± 0.16 | 0.87 ± 0.17 | 0.87 ± 0.17 | 0.87 ± 0.09 | 0.87 ± 0.09 |

| F1-score | Axon | | Dendrite | | Neurite | |
|-------------------------|-----------------|-----------------|-----------------|-----------------|-----------------|-----------------|
| Distance, μm | raw | masked | raw | masked | raw | masked |
| 2 | 0.66 ± 0.13 | 0.67 ± 0.13 | 0.74 ± 0.16 | 0.74 ± 0.16 | 0.80 ± 0.08 | 0.80 ± 0.08 |
| 5 | 0.75 ± 0.13 | 0.76 ± 0.13 | 0.78 ± 0.15 | 0.78 ± 0.15 | 0.87 ± 0.07 | 0.87 ± 0.07 |
| 10 | 0.82 ± 0.12 | 0.83 ± 0.12 | 0.83 ± 0.13 | 0.83 ± 0.13 | 0.92 ± 0.06 | 0.92 ± 0.06 |

Table S1: **Neuron reconstruction accuracy.** Precision, recall, and F1-score values are calculated by comparing automated and manual trace nodes within a given distance (2, 5, and 10 μm). Mean \pm s.d. of the values over $n=340$ cells are reported for axonal, dendritic, and neurite (combined axonal and dendritic) nodes of raw and masked automated traces. Source data are provided as a Source Data file.

| Precision | Axon | | Dendrite | | Neurite | |
|-------------------------|-----------------|-----------------|-----------------|-----------------|-----------------|-----------------|
| Distance, μm | manual | auto | manual | auto | manual | auto |
| 2 | 0.93 ± 0.02 | 0.88 ± 0.01 | 0.99 ± 0.00 | 0.82 ± 0.00 | 0.93 ± 0.02 | 0.91 ± 0.01 |
| 5 | 0.97 ± 0.01 | 0.92 ± 0.01 | 1.00 ± 0.00 | 0.86 ± 0.01 | 0.97 ± 0.01 | 0.94 ± 0.01 |
| 10 | 0.98 ± 0.01 | 0.95 ± 0.01 | 1.00 ± 0.00 | 0.89 ± 0.01 | 0.98 ± 0.01 | 0.96 ± 0.01 |

| Recall | Axon | | Dendrite | | Neurite | |
|-------------------------|-----------------|-----------------|-----------------|-----------------|-----------------|-----------------|
| Distance, μm | manual | auto | manual | auto | manual | auto |
| 2 | 0.92 ± 0.01 | 0.91 ± 0.01 | 0.98 ± 0.00 | 0.65 ± 0.00 | 0.92 ± 0.01 | 0.92 ± 0.01 |
| 5 | 0.96 ± 0.02 | 0.96 ± 0.01 | 0.99 ± 0.00 | 0.71 ± 0.00 | 0.96 ± 0.01 | 0.98 ± 0.01 |
| 10 | 0.97 ± 0.01 | 0.99 ± 0.00 | 0.99 ± 0.00 | 0.73 ± 0.00 | 0.97 ± 0.01 | 0.99 ± 0.00 |

| F1-score | Axon | | Dendrite | | Neurite | |
|-------------------------|-----------------|-----------------|-----------------|-----------------|-----------------|-----------------|
| Distance, μm | manual | auto | manual | auto | manual | auto |
| 2 | 0.92 ± 0.01 | 0.89 ± 0.00 | 0.99 ± 0.00 | 0.73 ± 0.00 | 0.93 ± 0.01 | 0.91 ± 0.00 |
| 5 | 0.96 ± 0.00 | 0.94 ± 0.00 | 0.99 ± 0.00 | 0.78 ± 0.00 | 0.97 ± 0.00 | 0.96 ± 0.00 |
| 10 | 0.98 ± 0.00 | 0.97 ± 0.00 | 1.00 ± 0.00 | 0.80 ± 0.00 | 0.98 ± 0.00 | 0.98 ± 0.00 |

Table S2: **Neuron reconstruction accuracy for multiple manual traces vs. the automated trace for a single test cell.** See Figure S15 for projections of the raw image and the corresponding reconstructions for this test neuron. Precision, recall, and F1-score values are calculated by comparing pairs of trace nodes within a given distance (2, 5, and 10 μm). Mean \pm s.d. of the values over three pairwise comparisons ($n=3$ pairs) are reported for axonal, dendritic, and neurite (combined axonal and dendritic) nodes of manual vs. manual traces and automated vs. manual traces. Source data are provided as a Source Data file.

| | Sst Calb2 Pdlim5 | Sst Hpse Cbln4 | Sst Chodl | Pvalb Reln Itm2a | Pvalb Tpbg | Lamp5 Lsp1 |
|-------------------|---------------------|---------------------|---------------------|---------------------|---------------------|---------------------|
| L1 axon | 0 / 0.40 | 1.000 | 0.637 | 0.023 / 0.13 | 0.033 / 0.21 | 0.013 / 0.56 |
| L2/3 axon | 0.013 / 0.30 | 1.000 | 1.000 | 0 / 0.35 | 0.023 / 0.27 | 0.042 / 0.52 |
| L4 axon | 0.689 | 0.332 | 0.607 | 0 / 0.35 | 0.216 | 1.000 |
| L5 axon | 0.033 / 0.15 | 0.013 / 0.25 | 1.000 | 0.102 | 0.058 | 0.135 |
| L6 axon | 1.000 | 0.081 | 0.288 | 0.182 | 1.000 | 0.058 |
| L1 dendrite | 0.042 / 0.17 | 1.000 | 0.689 | 0.088 | 0 / 0.42 | 0.283 |
| L2/3 dendrite | 0.033 / 0.15 | 1.000 | 0.332 | 0.013 / 0.27 | 0.042 / 0.21 | 1.000 |
| L4 dendrite | 0.697 | 0 / 0.40 | 0.013 / 0.40 | 0.058 | 0.074 | 0.393 |
| L5 dendrite | 0 / 0.19 | 0.102 | 0.393 | 0 / 0.25 | 0.013 / 0.26 | 1.000 |
| L6 dendrite | 1.000 | 0.088 | 0.866 | 0.051 | 0.363 | 1.000 |
| soma depth | 0 / 0.26 | 0.023 / 0.21 | 0.246 | 0 / 0.34 | 0.013 / 0.29 | 0.023 / 0.48 |
| axon centroid | 0.023 / 0.16 | 0.210 | 0.058 | 0 / 0.34 | 0.058 | 0.013 / 0.44 |
| dendrite centroid | 0.150 | 0.023 / 0.26 | 0.096 | 0 / 0.39 | 0.013 / 0.38 | 0.023 / 0.46 |
| | Lamp5 Plch2 Dock5 | Sst | Pvalb | Lamp5 | Vip | |
| L1 axon | 0.042 / 0.40 | 0 / 0.29 | 0 / 0.29 | 0 / 0.47 | 0 / 0.24 | |
| L2/3 axon | 0.322 | 0 / 0.41 | 0 / 0.66 | 0.813 | 0 / 0.27 | |
| L4 axon | 0.351 | 0 / 0.44 | 0 / 0.40 | 0.210 | 0 / 0.18 | |
| L5 axon | 0.081 | 0 / 0.33 | 0 / 0.21 | 1.000 | 0 / 0.18 | |
| L6 axon | 0.540 | 0 / 0.37 | 0 / 0.52 | 1.000 | 0.813 | |
| L1 dendrite | 0 / 0.40 | 0.023 / 0.01 | 0 / 0.42 | 0 / 0.25 | 1.000 | |
| L2/3 dendrite | 1.000 | 0 / 0.37 | 0 / 0.66 | 1.000 | 0 / 0.48 | |
| L4 dendrite | 1.000 | 0 / 0.42 | 0 / 0.28 | 1.000 | 0 / 0.16 | |
| L5 dendrite | 1.000 | 0 / 0.19 | 0 / 0.24 | 1.000 | 0 / 0.34 | |
| L6 dendrite | 1.000 | 0 / 0.44 | 0 / 0.59 | 1.000 | 0.689 | |
| soma depth | 0.067 | 0 / 0.48 | 0 / 0.70 | 0 / 0.24 | 0 / 0.33 | |
| axon centroid | 0.074 | 0 / 0.53 | 0 / 0.72 | 0 / 0.25 | 0 / 0.29 | |
| dendrite centroid | 0.074 | 0 / 0.45 | 0 / 0.68 | 0 / 0.26 | 0 / 0.21 | |

Table S3: **Statistical significance and effect size values for predicting anatomical features from gene expression via sparse linear regression for seven different cell types and four subclasses.** For each entry, the FDR-corrected p -value as calculated by a non-parametric one-sided shuffle test is listed. (See Sparse feature selection analysis under Methods.) If the value is considered statistically significant at $p \leq 0.05$, the R^2 value is also displayed (p / R^2). p -values less than or equal to 0.05 and R^2 values larger than or equal to 0.25 are shown in bold. Source data are provided as a Source Data file.

| | Sst Calb2 Pdlim5 | Sst Hpse Cbln4 | Sst Chodl | Pvalb Reln Itm2a | Pvalb Tpbg | Lamp5 Lsp1 |
|-------------------|---------------------|---------------------|---------------------|----------------------|---------------------|----------------------|
| L1 axon | 0 / 0.40 | 0.481 | 0.090 | 0.002 / 0.13 | 0.003 / 0.21 | 0.001 / 0.56 |
| L2/3 axon | 0.001 / 0.30 | 0.232 | 0.306 | 0 / 0.35 | 0.002 / 0.27 | 0.004 / 0.52 |
| L4 axon | 0.100 | 0.044 / 0.01 | 0.085 | 0 / 0.35 | 0.027 / 0.06 | 0.312 |
| L5 axon | 0.003 / 0.15 | 0.001 / 0.25 | 0.347 | 0.012 / 0.07 | 0.006 / 0.14 | 0.016 / -0.45 |
| L6 axon | 0.251 | 0.009 / 0.10 | 0.037 / 0.11 | 0.022 / -0.05 | 0.227 | 0.006 / 0.32 |
| L1 dendrite | 0.004 / 0.17 | 0.895 | 0.100 | 0.010 / -0.26 | 0 / 0.42 | 0.036 / -0.03 |
| L2/3 dendrite | 0.003 / 0.15 | 0.234 | 0.044 / 0.05 | 0.001 / 0.27 | 0.004 / 0.21 | 0.189 |
| L4 dendrite | 0.102 | 0 / 0.40 | 0.001 / 0.40 | 0.006 / 0.09 | 0.008 / 0.15 | 0.054 |
| L5 dendrite | 0 / 0.19 | 0.012 / 0.13 | 0.054 | 0 / 0.25 | 0.001 / 0.26 | 0.174 |
| L6 dendrite | 0.230 | 0.010 / 0.15 | 0.130 | 0.005 / 0.08 | 0.049 / 0.01 | 0.177 |
| soma depth | 0 / 0.26 | 0.002 / 0.21 | 0.031 / 0.06 | 0 / 0.34 | 0.001 / 0.29 | 0.002 / 0.48 |
| axon centroid | 0.002 / 0.16 | 0.026 / 0.04 | 0.006 / 0.26 | 0 / 0.34 | 0.006 / 0.21 | 0.001 / 0.44 |
| dendrite centroid | 0.018 / 0.18 | 0.002 / 0.26 | 0.011 / 0.22 | 0 / 0.39 | 0.001 / 0.38 | 0.002 / 0.46 |
| | Lamp5 Plch2 Dock5 | Sst | Pvalb | Lamp5 | Vip | |
| L1 axon | 0.004 / 0.40 | 0 / 0.29 | 0 / 0.29 | 0 / 0.47 | 0 / 0.24 | |
| L2/3 axon | 0.042 / 0.08 | 0 / 0.41 | 0 / 0.66 | 0.120 | 0 / 0.27 | |
| L4 axon | 0.047 / 0.01 | 0 / 0.44 | 0 / 0.40 | 0.026 / 0.01 | 0 / 0.18 | |
| L5 axon | 0.009 / 0.07 | 0 / 0.33 | 0 / 0.21 | 0.186 | 0 / 0.18 | |
| L6 axon | 0.075 | 0 / 0.37 | 0 / 0.52 | 0.177 | 0.121 | |
| L1 dendrite | 0 / 0.40 | 0.002 / 0.01 | 0 / 0.42 | 0 / 0.25 | 0.208 | |
| L2/3 dendrite | 0.218 | 0 / 0.37 | 0 / 0.66 | 0.510 | 0 / 0.48 | |
| L4 dendrite | 0.285 | 0 / 0.42 | 0 / 0.28 | 0.214 | 0 / 0.16 | |
| L5 dendrite | 0.217 | 0 / 0.19 | 0 / 0.24 | 0.217 | 0 / 0.34 | |
| L6 dendrite | 0.292 | 0 / 0.44 | 0 / 0.59 | 0.160 | 0.099 | |
| soma depth | 0.007 / 0.20 | 0 / 0.48 | 0 / 0.70 | 0 / 0.24 | 0 / 0.33 | |
| axon centroid | 0.008 / 0.23 | 0 / 0.53 | 0 / 0.72 | 0 / 0.25 | 0 / 0.29 | |
| dendrite centroid | 0.008 / 0.16 | 0 / 0.45 | 0 / 0.68 | 0 / 0.26 | 0 / 0.21 | |

Table S4: **Statistical significance and effect size values for predicting anatomical features from gene expression via sparse linear regression for seven different cell types and four subclasses – before FDR correction.** For each entry, original p -value as calculated by a non-parametric one-sided shuffle test is listed. If the value is considered statistically significant at $p \leq 0.05$, the R^2 value is also displayed (p / R^2). p -values less than or equal to 0.05 and R^2 values larger than or equal to 0.25 are shown in bold. Source data are provided as a Source Data file.

| Population | Feature | Genes |
|-------------------|-------------------|--|
| Sst Calb2 Pdlim5 | L1 axon | Cpn7 (5), Nercab2 (4), Crhr2 (4), Myh7 (4), Metrnl (3), Bcl11a (3), Ptpn1 (3), Atp2b4 (2), Elfn1 (2), Tmem163 (2) |
| Sst Calb2 Pdlim5 | L2/3 axon | Hs8s11 (5), Ekon5 (5), Mb21d2 (5), Cacng5 (3), Adrala (3), Fxyo7 (2), Pth2c (2), Ab4b (2), Symp (2), Sxt10 (2) |
| Sst Calb2 Pdlim5 | soma depth | Chr2 (5), Cari10 (4), Env1 (4), Gap43 (2), Igfbp6 (2), Klf8 (2), Neto2 (2), Galnt14 (2), Sgcez (2), Syt2 (2) |
| Sst Hpsc Chb4 | L5 axon | Timp2 (5), Fasgef1c (5), Shirk1 (4), Modag (3), Thfafpb13 (3), LOC102632463 (3), Lre38 (2), Gprin3 (2), Kcnip4 (2), Zbtb20 (2) |
| Sst Hpsc Chb4 | L4 dendrite | Kcnab1 (5), Rnab1 (5), Timp2 (4), Krt1 (4), Mme (3), Timp2 (3), Pipro (3), Map3k5 (3), Fxyd7 (2), Nrda2 (2), Cabra5 (2) |
| Sst Hpsc Chb4 | denrite centroid | Rasgef1c (5), Myh7 (4), Krt1 (4), Mme (3), Timp2 (3), Pipro (3), Map3k5 (3), Fxyd7 (2), Nrda2 (2), Cabra5 (2) |
| Sst Chodl | L4 dendrite | Col14a1 (5), 2010300c02Rik (4), Sema6d (4), Sema3a (3), Sema3e (2), Sem3e (2), Sema3e (2), Adcyap1rl (2) |
| Pvalb Rein Itm2a | L2/3 axon | Ncam2 (5), Sertad1 (5), Cort (5), Lrrtn4 (5), Thsd7a (5), Gaant6 (4), Grm7 (4), Kcnd3 (4), Npas3 (2), Nell2 (2) |
| Pvalb Rein Itm2a | L4 axon | Cdh9 (5), Cort (5), Braind (4), Netol (4), Cpx2 (4), Palml1 (3), Kenk1 (3), Ephb1 (2), Ndstd3 (2), Lxn (1) |
| Pvalb Rein Itm2a | L2/3 dendrite | Ctnn5 (5), Vax1 (5), Sertad1 (5), Kend3 (5), Loci10244192 (5), Cdhd1b (4), Gadd45a (4), Grkl (2) |
| Pvalb Rein Itm2a | L5 dendrite | Npas3 (5), Gaant6 (5), Kcnip4 (5), Brinp3 (5), Ncam2 (5), Kend3 (5), Loci10244192 (4), Ano3 (3), Cdhd1b (3), Caenca2d3 (2), Tox (2) |
| Pvalb Rein Itm2a | soma depth | Thsd7a (5), Npas3 (5), Brinp3 (5), Sartbl (5), Csgnahact1 (4), Spibn5 (4), Ankrd34b (3), Grm7 (3), Ncam2 (3), Kenjip4 (3) |
| Pvalb Rein Itm2a | axon centroid | Npas3 (5), Thsd7a (5), Tox (4), Spibn5 (4), Grm7 (4), Cdhd22 (3), Grkl (3), Opem1 (3), Sertad1 (2), Rgs6 (2) |
| Pvalb Rein Itm2a | dendrite centroid | Galnt16 (5), Spibn5 (4), Tox (4), Kcnip4 (3), Opem1 (3), Lrp1b (2), Kond3 (2) |
| Pvalb Tpbwg | L2/3 axon | Poc1a (5), Caenca1g (5), Matn2 (3), 9630002D21Rik (3), Fam46a (3), 8030453O22Rik (3), Wipf3 (2), Sfrp2 (2), Necab2 (2), Map3k5 (2) |
| Pvalb Tpbwg | L1 dendrite | Itpk1a (5), Nos1 (4), Npx2 (4), Grhl1 (3), Lypd1 (3), Cnih3 (2), Ifgl1 (2), Tesc2 (2), Zaril1 (2), Sel113 (2) |
| Pvalb Tpbwg | L5 dendrite | 9630002D21Rik (5), 8030453O22Rik (4), LOC105243512 (4), Slt10a4 (4), Sfrp2 (4), Cab1 (3), Cnd24a (3), Cmya5 (3), Dgkb (2), Hs3st2 (2) |
| Pvalb Tpbwg | soma depth | Col25a1 (4), 9630002D21Rik (3), BC048546 (3), Osbpl3 (3), Nxpsh1 (3), Myole (3), Ipkpa (2), Sfrp2 (2), Nt443 (2), LOC105243512 (2) |
| Pvalb Tpbwg | dendrite centroid | 9630002D21Rik (5), Nxpsh1 (3), Sfrp2 (3), Osbpl3 (3), Dgkb (3), Itpkpa (3) |
| Lamp5 Lsp1 | L1 axon | Dusp14 (5), March11 (5), Nptx1 (4), Sstr4 (3), Pon3t3 (3), Ndst4 (2), Gice (2), Pho43 (2), Meaf4c (2) |
| Lamp5 Lsp1 | L2/3 axon | Sertad1 (5), Sdk2 (4), Hunk (4), Sulf1 (4), Pbx3 (3), Teddin3 (2), Elav12 (2), 3500002P13Rik (2), Rorb (1), Raf152 (1) |
| Lamp5 Lsp1 | soma depth | Adrah1 (4), Sulf1 (4), Rnf152 (3), Pde1a (3), Dusp14 (2), Hdac9 (2), Idnr2 (2), LOC105243542 (2), Nog (2), Sic4a5 (2) |
| Lamp5 Lsp1 | axon centroid | Rnf152 (5), Adrah1 (4), Nog (3), Pde1a (3), Hdc4 (2), Rapigap2 (2), Dusp14 (2), LOC105243542 (2), Cpxix3 (1) |
| Lamp5 Lsp1 | dendrite centroid | Adrah1 (5), Sulf1 (4), Rnf152 (4), Pde1a (3), Hdc4 (2), Rapigap2 (2), Dusp14 (2), Idnr2 (2) |
| Lamp5 Pich2 Dock5 | L1 axon | Zbtb20 (4), Frd6 (4), Frd6 (4), Dner (4), Asap2 (3), Ctnn3 (3), Slaeb5 (2), Sel113 (2), Rgs8 (2), Open1 (2) |
| Lamp5 Pich2 Dock5 | L1 dendrite | Zbtb20 (5), Frd6 (5), Cankkg (5), Ngf (3), Prad1 (2), Tmod1 (2), Mitf (2), Thsd7a (2), Timp2 (1), Kenip1 (1) |
| Sst | L1 axon | Pesk1 (5), Myh7 (5), Mgat4c (5), Ketds8 (4), Olfm3 (4), Npx2r (4), Atp2b4 (4), Thsd7a (3), Ajap1 (2) |
| Sst | L2/3 axon | Grkl (5), Magat4c (5), Thsd7a (5), Rgs9 (4), Grkl (5), Rgs9 (4), Grkl (3), Ap1 (2), Co125al (2), Satb1 (2) |
| Sst | L4 axon | Tmem132d (5), Npnt (5), Hpsc (5), Sndg11 (5), Lrrtm1 (4), Pde9a (4), Cort (3), March1 (3), Rerg (2), Kenab1 (2) |
| Sst | L5 axon | Arc (5), Sema3e (5), Col11a1 (5), Grm1 (5), Sponi1 (4), Olfm3 (4), Lypd6 (4), Myh7 (3), Mgat4c (3), Map3k5 (2) |
| Sst | L6 axon | Col6a1 (5), Dpp10 (5), Grkl (4), Brinp3 (4), Car103 (4), Crys (4), Kirel3 (3), Penk (3), Sp8 (3) |
| Sst | L2/3 dendrite | Rgs9 (5), Npx2r (5), Chhn4 (5), Mgat4c (5), Ketds8 (4), Olfm3 (4), Npx2r (4), Atp2b4 (4), Thsd7a (2), Dab1 (2) |
| Sst | L4 dendrite | Sndg11 (5), Ptxpfb (5), Hpsc (5), Col11a1 (4), Semaze (4), Semaze (4), Gabrg3 (4), Epha3 (4), Grkl (3), Pde9a (2) |
| Sst | soma depth | Mgat4c (5), Olfm3 (5), Kirel3 (5), Sndg11 (5), Sndg11 (5), Lrrtm1 (4), Pde9a (4), Cort (3), March1 (3), Rerg (2), Kenab1 (2) |
| Sst | axon centroid | Kirel3 (5), Thsd7a (5), Olfm3 (5), Car103 (5), Mgat4c (5), Syndg1 (4), Brinp3 (4), Grkl (4), Unc5d (2) |
| Sst | denrite centroid | Olfm3 (5), Mgat4c (5), Thsd7a (5), Rgs9 (3), Brinp3 (3), Myh7 (3), Car103 (3), Grkl (3), Kirrel3 (3) |
| Pvalb | L1 axon | Igfl (5), Myh7 (5), Mgat4c (5), Col102636041 (5), 2010300C02Rik (4), Myb7 (4), Cl30074G10Rik (3), LOC102636041 (5), Itpkpa (3), Rgs14 (2), Cdha4 (2) |
| Pvalb | L2/3 axon | Grkl (5), Col6a1 (5), Olfm3 (5), Kirel3 (5), Sndg11 (5), Gaant6 (5), Gaant6 (5), Cnr1 (4), Pcp4 (4), Knc2 (2), Col25a1 (2) |
| Pvalb | L4 axon | Lrrtm4 (5), Parml1 (5), Cnnmap5c (4), Ntk3 (4), Ddn (4), Neto1 (3), Lin7a (3), Cdhd9 (2), Rasgfl (2), Gpr123 (1) |
| Pvalb | L6 axon | Chrm2 (5), Gaant6 (5), Sema3e (5), Prems8 (4), Rasgfl (4), Zips804b (3), Knc2 (2), Lrp1b (2), Brinp2 (2) |
| Pvalb | L1 dendrite | Igfl (5), Myh7 (5), Mgat4c (5), Ptxpfb (3), Igfbp6 (3), Ketds8 (3), Itpkpa (2), Adcyap1 (2) |
| Pvalb | L2/3 dendrite | Thsd7a (5), Ncam2 (5), Grkl (5), Gaant6 (5), Col25a1 (5), Cnr1 (5), Cab1 (5), Pcp4 (4), Cdhd13 (4), Ning1 (2) |
| Pvalb | L4 dendrite | Parml1 (5), Ntk3 (5), Chrn7 (3), St6galnac5 (3), Ctnnp5c (3), Grl123 (3), Grial (2), Lrrtn4 (2), Co125al (2), Trp13 (1) |
| Lamp5 | L1 dendrite | Temp2 (5), Fasgef1 (3), Tmt1 (3), Dner (3), Open1 (3), Pch2 (3), Zfp467 (2), Gabra5 (2), Lingo02 (2), Mittf (2) |
| Lamp5 | axon centroid | Islr2 (4), Rgma (3), Ceer6 (3), Sldca4a5 (3), Rtn4r (3), Rep1gap2 (3), Cpxix3 (2), Dner (2), Pch2 (2) |
| Lamp5 | denrite centroid | Sldca4a5 (4), Glt8d2 (4), Timp2 (3), Cee6f (3), Islr2 (3), Cpxix3 (3), Rgma (3), Cdca7 (2), Ruf152 (2), Oprml1 (2) |
| Vip | L2/3 axon | Kcnmb4 (5), Elmh1 (5), Isoc1 (5), Kirrel3 (4), Cdhd13 (4), Edtl3 (4), Knc2 (3), Fstl14 (3), Gpr83 (3), Lgs1 (2) |
| Vip | L2/3 dendrite | Symp (5), Kirel3 (5), Sndg1 (4), Sndg1 (4), Gapt43 (4), Eya4 (3), Sndg1 (4), Rgs14 (2), Chr3 (2), Cxcl14 (2) |
| Vip | L5 dendrite | Symp (5), Stp2 (5), Islr2 (5), Kirel3 (5), Kit (4), Col11a1 (4), Sndg1 (4), Rgs14 (2), Chr3 (2), Cxcl14 (2) |
| Vip | soma depth | Symp (5), Papdc1a (5), Kirel3 (5), Rhn1 (4), Kit (3), Chrm3 (3), Megf10 (3), Whrrn (2), Oskp3 (2), Eya4 (2) |
| Vip | axon centroid | Symp (5), Kirel3 (5), Kit (5), Rhn1 (4), Papdc1a (4), Rhn1 (4), Cnr1 (3), Umc5a (2), Cort (2), Eya4 (2) |

Table S5: Gene sets selected via sparse linear regression for different cell types/subclasses and anatomical features. Only statistically significant sets with $R^2 \geq 0.25$ are shown (See Supplementary Table 1). Numbers in parentheses denote the number of times the preceding gene was selected out of 5 cross-validation runs. Source data are provided as a Source Data file.